2024-12-18

Time Reversal Delivery of Long Duration Noise to a Targeted Location: Achieving Higher Amplitude While Maintaining a Desired Spectral Shape and Maximizing the Spatial Extent

Rylee Scott Russell
Brigham Young University

Time Reversal Delivery of Long Duration Noise to a Targeted Location: Achieving Higher Amplitude While Maintaining a Desired Spectral Shape and Maximizing the Spatial Extent

Rylee Scott Russell

A thesis submitted to the faculty of
Brigham Young University
in partial fulfillment of the requirements for the degree of

Master of Science

Brian E. Anderson, Chair
Micah R. Shepherd
Matthew S. Allen

Department of Physics and Astronomy

Brigham Young University

ABSTRACT

Time Reversal Delivery of Long Duration Noise to a Targeted Location:
Achieving Higher Amplitude While Maintaining a Desired
Spectral Shape and Maximizing the Spatial Extent

Rylee Scott Russell
Department of Physics and Astronomy, BYU
Master of Science

Time Reversal (TR) is a signal processing technique that can be used to focus acoustic waves to a specific location in space, with most applications aiming to create an impulsive focus. This study instead aims to focus long-duration noise signals using TR. This thesis seeks to generate higher amplitude noise at a desired location over an existing method of broadcasting equalized noise. Additionally, this thesis explores various characteristics associated with focusing long duration noise using TR. The dependence of the focal amplitude on the duration of the focused signal is explored as well as the implications of using multiple sources when focusing noise. The focal amplitude decreases with longer duration and then levels off when the duration exceeds a few seconds. Coherent addition of focused noise is observed if all loudspeakers have coherent noise signals convolved with their reversed impulse responses. Lastly, focusing noise with a desired spectrum is explored.

The use of audible sound for acoustic excitation is commonly employed to assess and monitor structural health, as well as to replicate the environmental conditions that a structure might experience in use. Achieving the required amplitude and specified spectral shape is essential to meet industry standards. The thesis seeks to understand the spatial dependence of focusing long-duration noise signals using TR to increase the spatial extent of the focus. Both one- and two-dimensional measurements are performed and analyzed using TR with noise, alongside traditional noise broadcasting without TR. The variables explored include the density of foci for a given length/area, the density of foci for varying length with a fixed number of foci, and the frequency content and bandwidth of the noise. A use case scenario is presented that utilizes a single-point focus with an upper frequency limit to maintain the desired spectral shape while achieving higher focusing amplitudes

Keywords: time reversal, long duration, steady state, spatial extent, multipoint

ACKNOWLEDGMENTS

I would like to express my heartfelt gratitude to my family and friends for their unwavering support throughout this journey. I am deeply thankful to all my mentors who have guided and inspired me over the years, with special thanks to Brian Anderson, Vern Hart, and Steve Wasserbaech. To everyone else who has offered support and encouragement, especially during challenging times, I sincerely appreciate your kindness and belief in me.

Special acknowledgments go, firstly, to Sandia National Laboratories for funding this project and making this work possible. Secondly, I would like to thank the BYU College of Computational, Mathematical, and Physical Sciences for providing additional funding and resources that were essential to carrying out my research.

TABLE OF CONTENTS

LIST OF FIGURES

LIST OF TABLES

Chapter 1

Introduction

Acoustical excitation is a well-established method for inducing vibrations in structures using sound waves.[1] Typically, a noise signal is broadcast from multiple loudspeakers to acoustically excite the structure. This technique is commonly employed in several testing scenarios (nondestructive evaluation/testing or structural health monitoring), such as detecting defects in a structure, conducting modal analysis, or testing the reliability of components under their intended use conditions. The latter is the main application of interest for the present research. The sound field must be at appropriately high sound levels to replicate the types of intense sound fields (dynamic fluid motion) that a structure might encounter when in use. For example, the turbulent sound field that a vehicle in flight experiences is caused by dynamic fluid motion imposed on the structure externally.

While assessments of structural vibration can be conducted using a shaker to induce vibration, this excitation technique serves its own unique purpose. For example, an engine mounted to the structure may directly induce structural vibration and in a case like this, excitation by a shaker would better replicate the source of the vibrations than would acoustic excitation. Using a shaker to vibrate smaller components poses challenges due to the need to mount the shaker onto the structure, which can alter the way the system responds.

Regardless of the reason for using acoustical excitation, a common problem is achieving the desired acoustic excitation amplitude. Some methods to reach high levels of excitation include increasing the gain on all the loudspeakers or using more loudspeakers and often using a reverberation chamber. Applications of the later case include creating cylindrical stacks of musical concert quality, modular loudspeakers that surround a structure under test (these setups can be done without a reverberation chamber). These approaches are typical for traditional excitation methods of broadcasting noise, sometimes including equalization of this noise to achieve a desired spectrum.

TR acoustics is a signal processing technique that harnesses not just the direct sound but also the reflections of acoustic waves to simultaneously focus energy to a single, selected point in space.[2,3] Instead of uniformly broadcasting acoustic waves throughout an environment containing a structure, TR harnesses the multiple reflected paths to provide coherent/constructive interference of sound that can excite a structure. This approach exploits multipath reflections to provide a gain in excitation amplitude relative to using traditional techniques with the same number of loudspeakers and the same amplifier gain settings. In applications of acoustical excitation of structures, the goal is to enhance excitation amplitude without increasing the number of loudspeakers or amplifier gain.

1.1 Thought Experiment Featuring a Racquetball Court

A thought experiment can help one understand how TR works. Imagine two individuals standing at opposite ends of a racquetball court. If Person A claps their hands, Person B will hear the initial "clap" followed by echoes bouncing off the walls, floor, and ceiling in the room. These

echoes are reflections of sound waves originating from Person A's clap but reaching Person B indirectly at various arrival times.

Now, consider what would happen if these sound waves were sent back along the same path they came, but in reverse order, with the latest reflection broadcast first, followed by earlier reflections, and finally the direct sound. In this scenario, Person A would perceive an impulsive-like clap sound (assuming conditions in the room don't change when these reversed sounds are played). This would occur because all the waves would meet at Person A simultaneously (all the reflected sounds traveled the same paths, just in reversed timing order), focusing energy at a single point space at an instance in time.

A practical approach to achieve this impulsive-like sound at Person A involves replacing Person A with a loudspeaker and Person B with a microphone. This process can be understood with the help of Fig. 1.1. The microphone records what Person B hears, capturing the initial clap (direct sound denoted by 1) and subsequent reflections (reflection paths denoted by 2 and 3). This is known as the forward step. By reversing this recorded signal in time, a new signal is created that plays the latest reflections first, followed by earlier reflections, and finally the direct sound. This is known as the backward step. In the backward step of Fig. 1.1, reflection path 3 would be broadcast first, followed by reflection path 2, and finally the direct sound. Additionally, utilizing the principle of reciprocity, the microphone can be replaced with a loudspeaker. When the loudspeaker broadcasts this reversed signal, the sound waves focus back to Person A, causing them to perceive a loud impulsive-like sound.

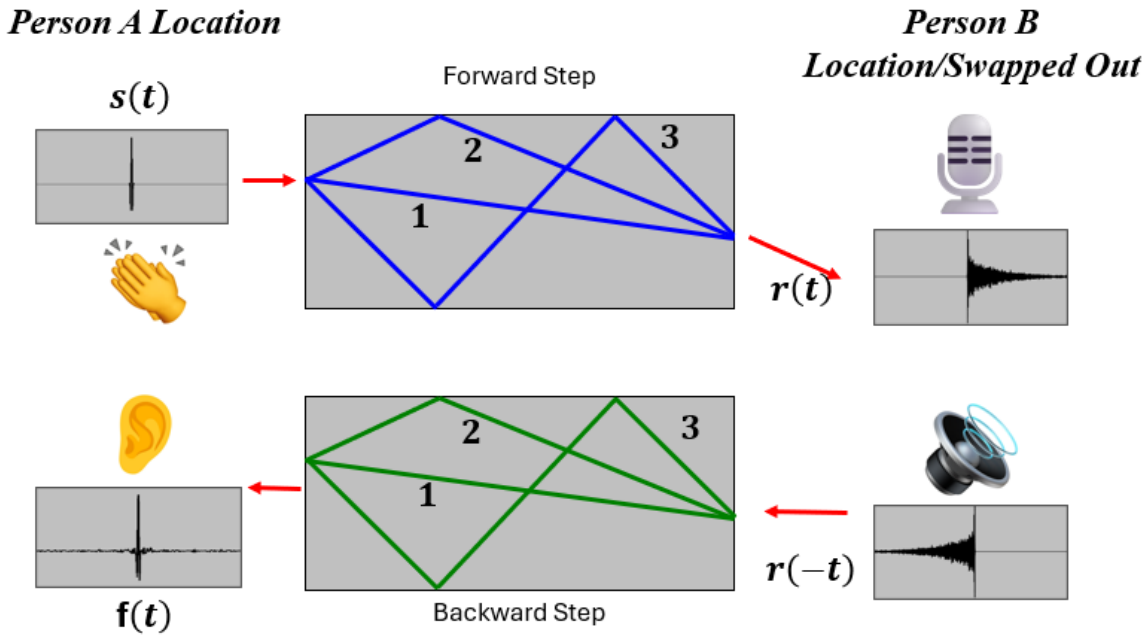

FIG. 1.1. Illustration of the time reversal process, starting with clapping in a room s(t). The microphone records the response of the clap, $r(t)$, (forward step). The clap recording is reversed in time, $r(-t)$, followed by its broadcast to result in a focus signal, $f(t)$, (backward step).

1.2 Experimental Implementation of TR in Acoustics

As introduced earlier, TR is a technique used to simultaneously focus acoustic wave energy to a single point in space at a specific moment in time. TR experiments can be performed in many environments as long as it's a linear, time-invariant system. For this thesis, TR is performed in a reverberation chamber, which is a highly reverberant environment, much like a racquetball court. TR has a greater effect in environments with longer reverberation times which create results ending in higher amplitudes than a direct flight of sound alone.[5,6]

To perform a TR experiment, a time-reversed impulse response (TRIR) needs to be obtained. A TRIR is essential for focusing sound. Although it may not have been intuitive, a TRIR was used in the previous section of the racquetball example. The recording of the clap with the direct sound followed by the reflections is considered an impulse response (IR). When an IR is reversed in time, it becomes a TRIR. In the thought experiment, using a clap to obtain an IR, $h(t)$, is acceptable because the response, $r(t)$, to an impulsive input, $s(t)$, is $h(t)$. However, in practical experiments, this is not the typical method for calculating an IR.

In experimental practice, a loudspeaker and microphone are used to obtain an IR. The loudspeaker and microphone can be placed anywhere in the chamber to obtain an IR, though their positions need to be maintained for both the forward and backward steps. This allows the loudspeaker to focus sound to the microphone location. However, if the loudspeaker is moved from the location where the IR was calculated, the loudspeaker will no longer focus sound to the microphone or anywhere in the room. The microphone and loudspeaker can switch locations and still obtain focusing due to reciprocity, but this is not typically done experimentally. In other words, in most TR implementations the sound is broadcast from A to B for the forward step and A to B for the backward step, which has been termed reciprocal TR,[3] as show in Fig. 1.2.

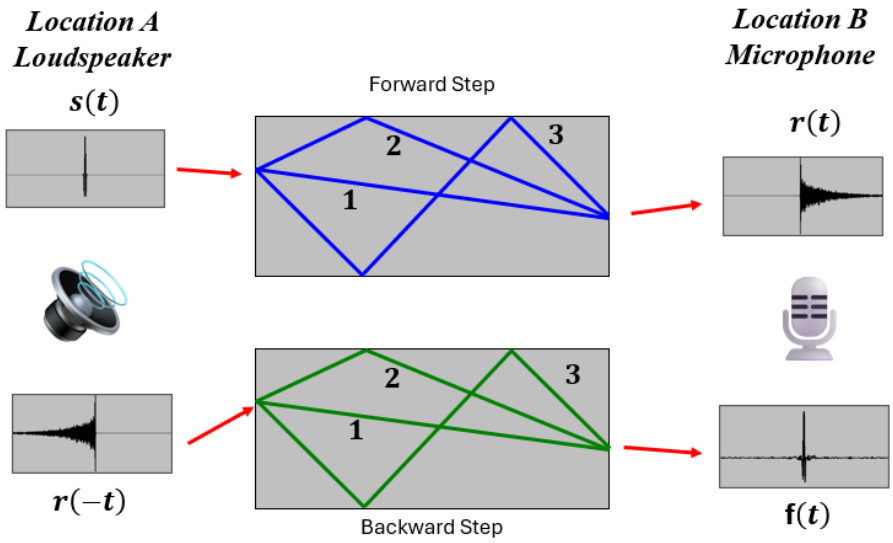

FIG. 1.2. Illustration of the reciprocal time reversal process involving broadcasting both the forward and backward signals into a room from the same location and the recordings are both made at a different location.

Once the loudspeaker and microphone locations have been chosen, a high-quality method to obtain an IR involves broadcasting a swept sine wave (chirp) containing a desired frequency bandwidth and recording at the microphone. The response of the broadcast chirp is called a chirp response. By applying cross-correlation, a signal processing technique, between the chirp and its response, the IR can be extracted.[4] Reversing the IR in time to get the TRIR and broadcasting it will result in an impulsive like focus. When multiple loudspeakers are used, every loudspeaker needs to be used in this process to calculate their own TRIR to focus sound.

For this thesis, impulsive focusing is not the goal; instead, focusing noise signals is the goal. This requires an additional step. By taking the desired noise signal to be delivered to a target location and convolving it with a TRIR, the noise signal can be focused at the target microphone

location. Figure 1.3 demonstrates the process of impulsive focusing (top route) and focusing noise signals (bottom route).

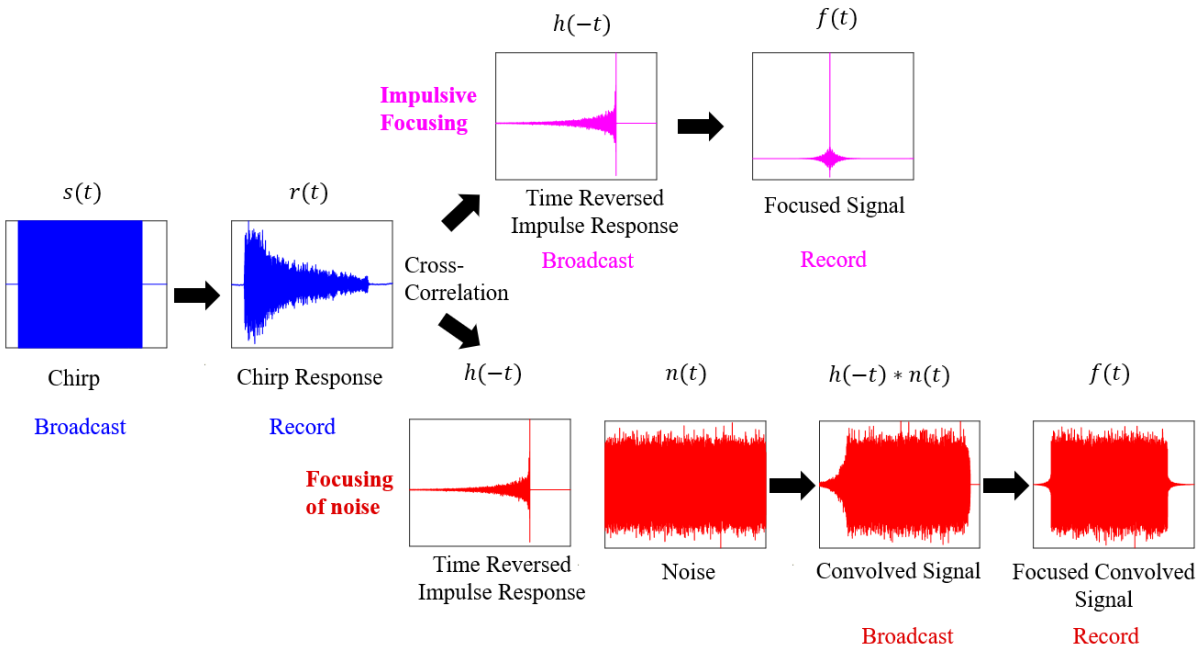

FIG. 1.3. A visual illustration of example signals used at each of the steps taken to obtain a focused impulse (top row) versus focusing noise (bottom row).

1.3 Outline

The purpose of this thesis is to help understand how TR works with focusing noise signals. The results and outcomes of this research will help improve upon methods to achieve acoustical excitation of structures by reaching a higher amplitude excitation without using higher amplifier gain or more loudspeakers. Applications may include finding defects in a structure, conducting modal analysis, or testing the reliability of components under their intended use conditions.

The second chapter explores focusing to single location and studies three characteristics. The first is focusing different durations of noise to see what effect it has on the amplitude. The second is exploring the effects of changing the total number of loudspeakers used to focus sound. The final characteristic is focusing a desired spectrum. This chapter represents a journal article manuscript that is intended to be submitted very soon, of which Russell is the first and primary author with Anderson as a coauthor.

The third chapter explores the spatial extent of focusing noise signals to one or more focal locations. The first part of this chapter examines the effects of varying the spacing between multiple focus locations while keeping the number of foci fixed. The second part, closely related to the first, investigates how changes in the density of multiple focus locations over a fixed length affects the combined focusing. Both parts will be analyzed in one dimension (1D), while the fixed length with varying numbers of foci will also be explored in two dimensions (2D). Both 1D and 2D experiments will be analyzed within the frequency domain. The objective is to observe how the spectral shape, including relative amplitudes, is influenced by these variables and to understand the frequency dependence of these changes. Based on the findings from the first two parts, a practical use case will be examined that could potentially be applied in the field of acoustic excitation to induce vibrations on a structure, resulting in a higher excitation level compared to existing methods. This chapter represents a second journal article manuscript that is intended to be submitted after the first one is accepted for publication, of which Russell is the first and primary author with Anderson as a coauthor, and including an undergraduate student Cliftmann for a small contribution he helped with.

Chapter 4 provides conclusions for the overall work of this thesis research and some ideas and suggestions for potential future work.

1.4 References

[1] Ono, K. Review on structural health evaluation with acoustic emission. Applied Sciences, **8**(6), 958 (2018).

[2] M. Fink, "Time reversed acoustics," *Phys. Today* **50**(3), 34-40 (1997).

[3] B. E. Anderson, M. Griffa, C. Larmat, T.J. Ulrich, P.A. Johnson, "Time reversal". *Acoust. Today* **4**(1), 5–16 (2008).

[4] B. E. Anderson, M. Clemens, and M. L. Willardson, "The effect of transducer directionality on time reversal focusing," J. Acoust. Soc. Am. **142**(1), EL95–EL101 (2017).

[5] G. Ribay, J. de Rosny, and M. Fink, "Time reversal of noise sources in a reverberation room,"*J. Acoust. Soc. Am.* **117**(5), 2866-2872 (2005).

[6] M. H. Denison and B. E. Anderson, "Time reversal acoustics applied to rooms of various reverberation times," *J. Acoust. Soc. Am.* **144**, 3055-3066 (2018).

Chapter 2

Using time reversal with long duration broadband noise signals to achieve high amplitude and a desired spectrum at a target location

Time Reversal (TR) is a signal processing technique that can be used to focus acoustic waves to a specific location in space, with most applications aiming to create an impulsive focus. This study instead aims to focus long-duration noise signals using TR. This paper seeks to generate higher amplitude noise at a desired location over an existing method of broadcasting equalized noise. Additionally, this paper explores various characteristics associated with focusing long duration noise using TR. The dependence of the focal amplitude on the duration of the focused signal is explored as well as the implications of using multiple sources when focusing noise. The focal amplitude decreases with longer duration and then levels off when the duration exceeds a few seconds. Coherent addition of focused noise is observed if all loudspeakers have coherent noise signals convolved with their reversed impulse responses. Lastly, focusing noise with a desired spectrum is explored.

2.1 Introduction

Time Reversal (TR) is a technique used in various applications to precisely focus sound waves in space for different purposes.[1,2] TR was first attempted in the 1960's in a coffee room by Clay and his colleagues[3]. They referred to TR at the time as matched signal processing. After the coffee room experiment, TR was implemented and used for underwater communication.[1,3] TR has been used in other fields such as communication in air,[4, 5] biomedical,[1,6] nondestructive evaluation.[2,7,8] and geophysics.[9,10] Normally TR is used to focus an impulsive sound or short duration noise signals, [2,11] whereas here we explore TR with long duration noise signals.

The TR process to focus an impulse consists of the following steps. The first step, commonly referred to as the forward step, is calculating or measuring an impulse response (IR). An IR can be measured using a loudspeaker and microphone. The IR can be determined by playing a swept sine wave (chirp) from the loudspeaker and recording the chirp response at the microphone. A cross correlation between the chirp and chirp response will result in a calculated IR.[12,13] Cross correlation is used in this paper because it results in a higher quality IR due to a higher signal to noise ratio excitation.

The second step, commonly referred to as the backward step, can be carried out now that the IR is obtained. Reversing the IR results in a time reversed impulse response (TRIR). The TRIR can then be broadcast from the same loudspeaker location. Broadcasting this TRIR time aligns the emission of all the reflections to constructively interfere at the microphone location, resulting in an impulsive focus. This can be modeled as an autocorrelation of the IR.[14] Focusing will occur even if the microphone and loudspeaker locations are interchanged and the same TRIR is used. Thus, broadcasting from position 1 to position 2 or position 2 to position 1 will have the same

result due to spatial reciprocity of a linear, time invariant system. Note that the concept of impulsive focusing described here has been used for ease of understanding, since the goal of the present work is focus long duration noise signals.

Candy *et al.*[4] conducted experiments in a highly reverberant room using TR transceivers and found that they can operate effectively in such environments, enabling the detection and recovery of transmitted information with zero errors. Ribay *et al.*[11] explored TR of noise signals in a reverberation chamber and found that the number of loudspeakers used is directly proportional to the signal to noise ratio of the focus signal. They defined their signal to noise ratio as the time averaged intensity at the focus location compared to locations elsewhere in the room. Denison *et al.* [15] also conducted TR simulations in various rooms and experiments in a variable size room and found that decreasing the volume and absorption of a room increases the focal amplitude and spatial clarity, which evaluates the temporal significance of focusing at one location compared to other locations, but decreases temporal quality, a measure of how closely the focal signal approximates a delta function, representing a high peak amplitude relative to surrounding noise. Furlong *et al.* [16] explored using active noise control and TR to reduce MRI noise by focusing opposite-phase signals at desired control points to achieve noise cancellation. The research explored varying pulse lengths and frequencies for noise reduction and transitions to using recorded MRI noise for proof-of-concept demonstrations.

Yon *et al.*[17] has shown that the number of loudspeakers used for TR focusing of audible sound in a room decreases the diameter of the spatial extent of the focusing (focus spot diameter). Apart from the spatial extent, the increasing number of loudspeakers decreases the relative amplitude at locations away from the focal location compared to the focal amplitude. When more loudspeakers are used there is some overall increase in amplitudes everywhere in the room, but the gain at the

location of the focused amplitude increases more than at other room locations, proportional to the number of loudspeakers used. It was also pointed out that for sound focused with TR in a reverberation chamber, the focus spot diameter does not depend on the number of loudspeakers if TR is being performed a reverberation chamber with a sufficient number of image sources (utilizing a long enough impulse response). Instead, the diameter is governed more strongly by the center frequency in the bandwidth used.[17]

Willardson *et al.*[18] explored generating high amplitude focusing of audible sound by using a TR method called clipping, achieving a peak focal amplitude of 173.1 dB. Patchett *et al.*[19] furthered these TR efforts to achieve a higher peak focal amplitude of 200.6 dB by using a logarithmic chirp instead of a linear chirp, pointing the loudspeakers away from the focal location,[12] focusing to a corner of the room,[20] and using clipping. That focal amplitude was approximately 2 times higher than linear scaling would suggest it would be due to the formation of free-space Mach stems that nonlinearly increased the peak amplitude of the focusing.[21] The experiments of both Willardson *et al.* and Patchett *et al.* were performed in a reverberation chamber. Wallace *et al.*[22] also studied the use of clipping in focusing airborne ultrasound in a reverberation chamber and explored nonlinear mixing of sound at high amplitudes.

Tanter *et al.*[14] found that TR focusing through a skull can be problematic due to the presence of spatial sidelobes at the focus, where sidelobes refer to secondary peaks in the pressure amplitude distribution that appear outside the main focus region during time-reversal wave focusing. They demonstrated that applying an inverse filter in conjunction with the TR process effectively reduces these sidelobes. Similarly, Ulrich *et al.*[23] and Anderson *et al.*[24] have shown that deconvolution, or inverse filtering, leads to a tighter spatial focus of an impulse. Montaldo *et al.*[25] introduced an innovative iterative time-reversal method that enables real-time acoustic focusing through

complex media without the need for extensive computation. This method effectively converges to the optimal inverse filter, providing high-quality focusing comparable to traditional numerical techniques but with greater efficiency and speed. It is important to note that while deconvolution or inverse filtering offers benefits such as a tighter focus and a flatter frequency response, resembling the spectrum of a delta function, these advantages come with the trade-off of a lower amplitude compared to the process without inverse filtering.

There has been research done by others to generate focused sound using TR in order to excite structures. Le Bas *et al.*[26] developed a noncontact acoustic source of impulsive, airborne ultrasound to excite vibration in a structure using TR in an enclosed cavity. Later they used this source to locate a crack and a delamination in a carbon fiber plate.[27] Farin *et al.*[28] focused audible, airborne sound using TR to acoustically excite complex structures and measure a frequency response. This technique allowed for selective excitation of a specific plate within a group, even when they are closely spaced and embedded in a complex structure. Farin *et al.*[29] furthered used this technique to remotely evaluate the eigenfrequencies of individual fan blades without disassembly, enabling precise detection of millimeter-sized damage.

In contrast to most previous studies, which used impulsive TR to excite structures and calculate frequency responses, this paper explores TR focusing of long-duration noise. The long-term goal is to use these techniques to excite structures in a manner that not only creates certain acoustical conditions, such as those experienced by a vehicle during takeoff, but does so at a higher amplitude than would be achieved by simply broadcasting noise.

Some work has been done exploring TR of long duration signals. Ribay *et al.*[11] showed that focusing of audible noise signals in a room is feasible. Through a combination of numerical simulations and experimental data the paper studied many factors. One being the signal-to-noise

ratio (SNR) for TR with noise signals and found that SNR is primarily dependent on the number of transducers, N, employed. Additionally, for the loudspeakers to contribute effectively to the SNR, they must be separated by at least one wavelength; otherwise, they function as a single element, diminishing the potential improvement in SNR. The paper also found that the focal spot width of noise is a half a wavelength of the central frequency in the bandwidth. They also studied the ability to resolve two closely spaced noise sources using both correlated and uncorrelated noise signals. This paper claimed that the peak energy in the TR focusing of pulses increased as N^2, with longer reverberation time of the room, and with larger bandwidth of the signal used. Anderson *et al.*[30] found similar results when applying TR with single-frequency, steady-state focusing of ultrasound in solids. They found that spatial focusing of a steady-state, single frequency is possible only if multiple sources are used. The energy of the focusing went up as N^2 at the focus location and went up by N at other spatial locations (spatial fringes).

This paper delves deeper into the use of TR with noise signals. Unlike the emphasis by Ribay *et al.*[11] and Anderson *et al.*[30] on SNR, resolution limits, and the ability to resolve two TR foci, the purpose of this paper is to investigate the relationship between the duration of the focused noise and the amplitude of that noise, explore the frequency-dependence of the coherent addition provided by multiple loudspeakers, and propose a method to achieve a desired spectrum in the focused noise signal. The traditional inverse filter process inherently aims to create a focus that is spectrally white, but we show here how the inverse filter may be used to focus noise that is intentionally not spectrally white. Higher overall sound pressure level (OASPL) values were obtained with shorter duration focused noise signals. While Ribay *et al.*[11] and Anderson *et al.*[30] both touched on the concept of coherent addition, they did not explicitly discus the coherent addition offered by TR for noise when using multiple sources, and instead used focused pulses and

single frequencies when reporting coherent addition. While all the present studies involve TR, a comparison will be made between the TR method and broadcasting noise to explore the amplitude gains possible when using TR. Both methods incorporate equalization in generating noise at the desired target location in the room.

2.2 Experimental details

2.2.1 Setup

The data is collected by performing experiments in the reverberation chamber at Brigham Young University. The dimensions of the chamber are 4.96 m × 5.89 m × 6.98 m resulting in a volume of 204 m^3. The reverberation time of the chamber is 7.6 s with a Schroeder frequency of 410 Hz.[19,31] The reverberation chamber also has diffuser panels hung from the ceiling. Mackie loudspeakers (HR824mk2 model) are used to broadcast all signals for the experiments. The loudspeakers are placed on stands facing the nearest wall, about 0.15 m away, to minimize the direct sound path amplitude. This is beneficial to obtain higher focal amplitudes when broadcasting a normalized TRIR.[12] Placing the loudspeakers too close alters the radiation impedance and potentially could overload the loudspeakers' amplifiers. A single G.R.A.S. 1.27 cm (0.5 inch) pre-polarized, random-incidence microphone (model 46AQ) is used for all experiments. The pre-polarized microphone is powered by a G.R.A.S. 12AX signal conditioner. The sensitivity of the microphone is 53.03mV/Pa. The microphone is always placed at least 1 m away from the wall to abide by the ISO standard to be in the diffuse field for measurements.[32] Another reason why the

microphone was placed 1 m from the wall was to prevent a doubling a pressure when focusing near a wall.[20] Figure 2.1 displays a photograph of the experimental setup in the reverberation chamber.

A custom LabVIEW™ program called Easy Spectrum Time Reversal (ESTR) is used to carry out the experiments.[33] ESTR is coupled to Spectrum (Grosshansdorf, Germany) M2i.6022 and M2i.4931 signal generation and digitizer cards, respectively. The use of ESTR in conjunction with this hardware provides several important capabilities. The first being able to broadcast and record multiple time-synced signals. The synchronous timing of the broadcast of multiple signals is crucial to have the TR process perform properly with multiple source channels. Besides broadcasting and recording signals, ESTR can also generate signals such as a chirp. ESTR can also be used to import user-defined signals. In this discussion, unless otherwise stated all imported signals are created in MATLAB.

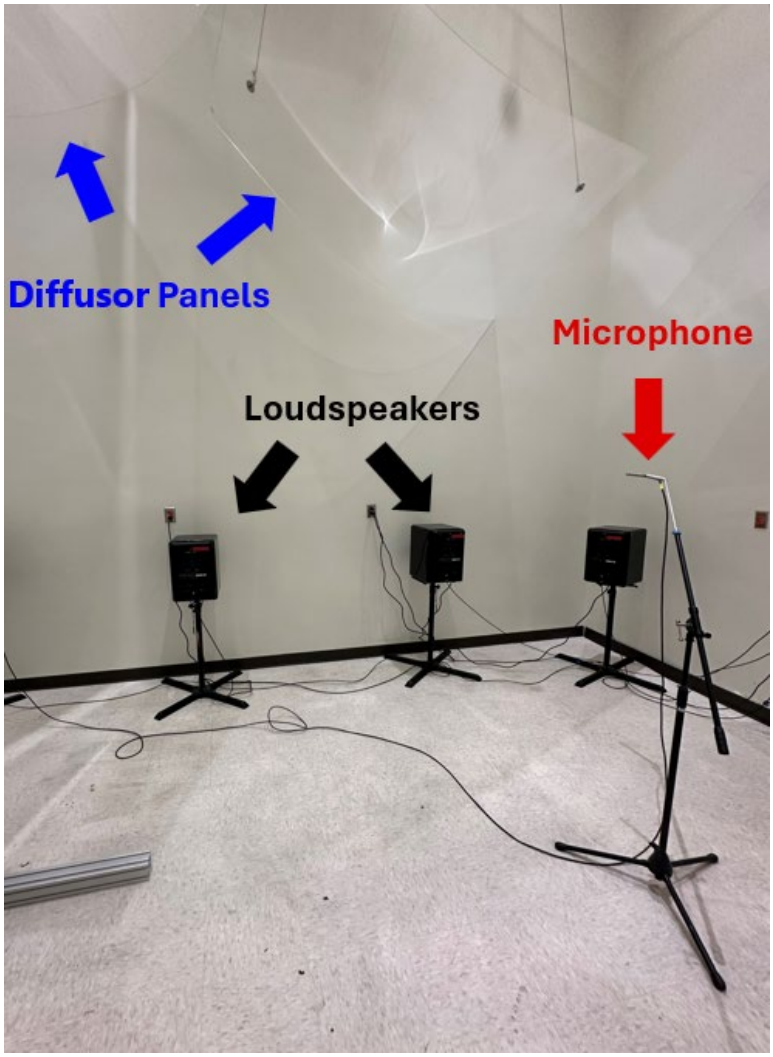

FIG. 2.1. Photograph of the experimental setup of the reverberation chamber consisting of diffusor panels (blue arrow), the loudspeakers (black arrows), and the microphone (red arrow). The positions of the loudspeakers and microphone shown are for visualization only and are not necessarily the same for all the experiments.

2.2.2 Time reversal with broadband noise

Once the hardware was set up, an impulse response was obtained between each loudspeaker and the microphone. The frequency responses of both the loudspeaker and the microphone are included in the impulse response. However, it is assumed that the frequency response of both is flat, based on the manufacturer's specifications. The TR process starts by broadcasting a linear swept sine wave (chirp), $s(t)$, one-by-one from every loudspeaker while the microphone records the corresponding chirp response, $r(t)$. The chirp broadcasts were not simultaneous since the individual impulse responses between each loudspeaker and the microphone are needed for TR. The chirp and the chirp response were exported for further processing in MATLAB and the IR, $h(t)$, was calculated using a cross-correlation operation[12] and reversed in time to obtain the TRIR, $h(-t)$. Broadcast of these TRIRs leads to impulsive focusing. The goal here is focusing long-duration noise signals, which requires that the TRIRs be convolved (denoted by $*$) with broadband noise, $n(t)$, prior to their broadcast. Figure 2.2 shows example signals used in both impulsive and broadband noise focusing, $f(t)$.

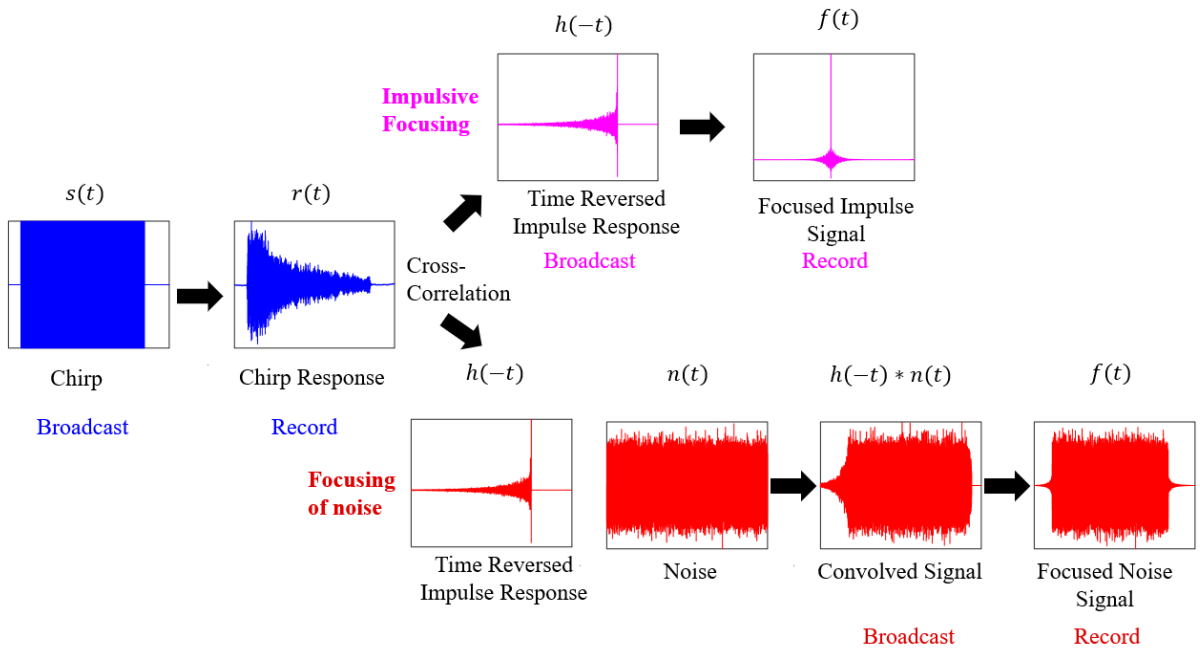

FIG. 2.2. A visual illustration of example signals used at each of the steps taken to obtain a focused impulse (top row) versus focusing noise (bottom row).

2.2.3 Equalization process of broadcasted signals

Equalizing the convolved signals (noise and TRIRs) before broadcasting is essential for creating a desired spectrum at the focal location. Standards specify certain spectra of acoustical noise be present at a location where a structure may be placed for acoustic load testing. Equalization involves compensating for the effects of room modes, propagation losses, and frequency-dependent absorption during propagation. Equalization is necessary to compensate, not only for an uneven transfer function during the forward step, but also to compensate for the expected similarly uneven transfer function that will occur during the backward step.

This process involves equalizing an IR in a manner that ensures any intended noise spectra convolved with the equalized IR results in the desired noise signal spectra at the target focal location. The equalization process is performed in the frequency domain. A Fast Fourier Transform (FFT) of the IR is performed to obtain a transfer function, which is then split into magnitude and phase components. Modifications are applied to the magnitude while preserving the phase, as the phase is pivotal for TR focusing of sound waves. An inverse filter is applied, but with some modifications. Half of the inverse filter (HIF) refers to equalizing a transfer function to compensate for a singular broadcast step attenuation. This HIF is quantified from the magnitude disparity between the flat-frequency response chirp signal and the chirp response signal, which has undergone filtration within the room environment. To achieve the desired spectral shape, the magnitude of the transfer function must be adjusted twice by the HIF to compensate for both the forward and backward steps. The phase is reattached at the end of the equalization process. It is worth noting that the broadcasting of noise without TR must have the HIF applied once, anticipating going through the system one time. HIF is a division of the chirp and chirp response spectral magnitudes,

$$x_{HIF} = x_{chirp}/x_{chirp\,response}. \tag{2.1}$$

If this initial HIF spectrum is multiplied twice by the transfer function, it is equivalent to the inverse filter. The problem with this inverse filter (essentially $\frac{1}{x}$) is that it unintentionally amplifies background noise, hence the need to modify the inverse filter, to achieve a higher maximum amplitude during the backward step.

The main purpose of the HIF spectrum from Eq. (1) is to increase the output amplitude of "inefficient frequencies" that were attenuated more than others. The high amplitude output at these

inefficient frequencies will again inefficiently transmit from the source to the receiver, thus setting a low *overall* achievable amplitude of the focusing. If we instead reduce the peaks in the HIF spectrum (the peaks are at these inefficient frequencies) relative to the rest of the spectrum we can achieve an overall gain in amplitude, resulting in a more efficient transmission to the focus location. The tradeoff is that those inefficient frequencies end up not having the same amplitude as the rest of the frequencies in the spectrum of the TR focusing. Similarly, Tanter *et al.*[14] uses a single value decomposition (SVD) method to avoid large errors caused from small errors in the system. SVD in this case is used to filter out the unwanted noise of the signal in what they call the inverse diffraction operator. Anderson *et al*.[24] added a finite number to the denominator of the $1/x$ inverse filter so that if x were ever a very small value, the finite number would limit the amplitude of the peaks. Thus, our implementation of regularization aims to achieve the same goals as others have done but it is implemented slightly differently.

Regularization will be applied to the spectrum in Eq. (1) to reduce the peak amplitudes of inefficient frequencies. The regularization process starts off by splitting up the spectrum into its corresponding 1/3rd octave band frequencies. The median (Pa/V)^2 amplitude value for each of these bands is determined. If any of the frequency amplitudes within the corresponding band are higher than the median amplitude for that band, they are reduced and set equal to the value of the median amplitude. This 1/3rd octave band level regularization seems appropriate since the overall goal is to generate levels at the focal location that are within a 1/3rd octave band specification standard. Figure 2.3 shows example spectra before and after the regularization has been applied on linear and logarithmic scales. Notice between 9 kHz and 10 kHz there is a major spike in amplitude for a particular inefficient frequency, roughly 7×10^7 (Pa/V)^2 in amplitude, which is 1-2 orders of magnitude larger than the rest of the spectrum. The significant amplification of this inefficient

frequency means that a lot of the finite available energy that could be broadcast from the loudspeaker at other frequencies will instead be broadcast at this frequency, which will again result in an inefficient transmission of amplitude to the microphone location. After regularization, the highest peak values are reduced to a value of 400 $(Pa/V)^2$. This regularized HIF spectrum is multiplied twice by the original transfer function spectrum and the phase information of the original transfer function is unmodified to create the final modified inverse filter (MIF). Applying an inverse FFT to the MIF results in an equalized impulse response. Reversing the equalized impulse response, denoted MIF TRIR, convolving it with noise, and subsequently broadcasting this convolution signal will result in focused noise with a spectral shape like that of the noise signal used.

To broadcast equalized noise, the HIF (with regularization) is multiplied once by the spectrum of the same noise used in the TR process. After this multiplication, an inverse FFT is used to convert the result back into the time domain, yielding the signal to be broadcast. The broadcast of this equalized noise signal will result in noise at the target location that has the desired spectrum, but no TR focusing is used in this process. This allows a fair comparison between when TR focusing is used versus not using TR, where both methods result in noise of the desired spectrum and utilize similar equalizations.

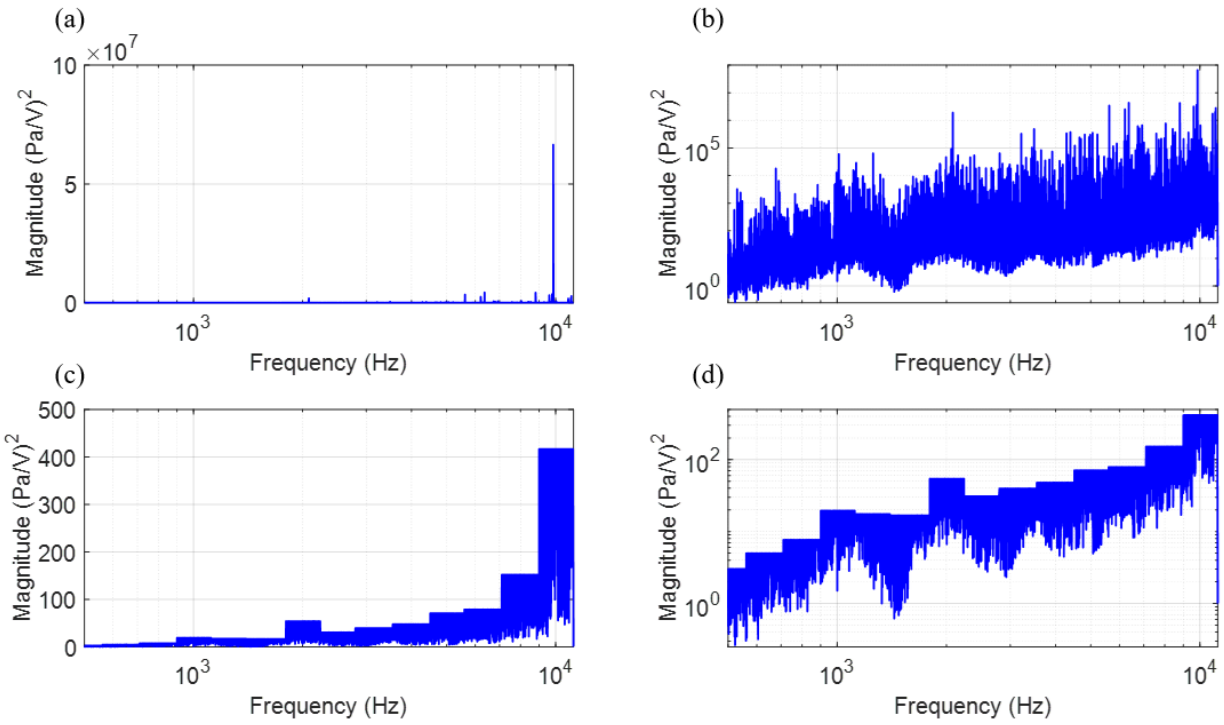

FIG. 2.3. These example plots show the transfer function of the chirp response spectrum before regularization on a linear scale (a) and a logarithmic scale (b), followed by the "half of the modified inverse filter" spectrum after regularization on a linear scale (c) and a logarithmic scale (d).

2.3 Experimental Results

2.3.1 Duration of focusing versus overall amplitude

The impact of the noise signal's duration on the amplitude of the focused noise when using TR will now be explored. Different durations of noise with the same bandwidth of 560 Hz to 11.2

kHz were focused to the same microphone location using six loudspeakers, with each loudspeaker creating focusing of identical noise signals. The noise duration was varied between 10 ms and 20 s. For reference an “impulsive TR focus” experiment was also conducted (technically it is a band limited impulsive focus), meaning no noise was convolved with the impulse response. The peak focal amplitude of this band limited impulsive noise is observed at the 0.4 ms tick mark (corresponding to its finite time span) and is labeled as 'Impulse'. This peak amplitude has been converted into a root mean square (RMS) value to represent the peak focal amplitude. The OASPL for the focal results that have a finite time duration is calculated in the time domain as

$$OASPL = 10\log_{10}(\overline{p(t)^2}/P_{ref}^2), \tag{2.2}$$

where $\overline{p(t)^2}$ is the mean squared pressure over time and P_{ref} is a RMS reference pressure of $20\ \mu Pa$. The calculation of the OASPL only utilizes the steady state portion of the time signal. For example, referring to Fig. 2.4, the steady-state portion of the 5 s duration focus is portrayed between the red dashed lines at 2 s and 7 s is used in calculating the OASPL (the ramp-up and decay transients are not included). This process is used for all other durations of focusing.

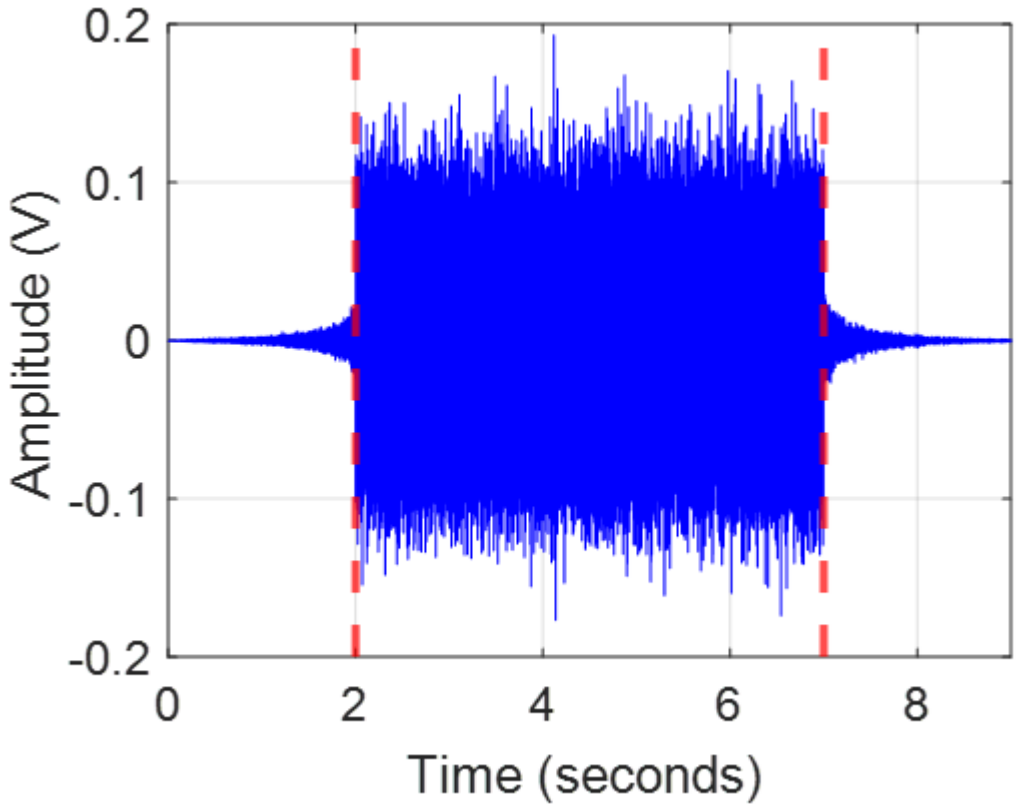

FIG. 2.4. An example focal signal with the steady-state portion existing between the red-colored, dashed, vertical lines, located at 2 s and 7 s.

The results show that the duration of the focused noise has an impact on the time-averaged amplitude. Figure 2.5 shows that the OASPL decreases with an increasing duration of the focused noise signal. The maximum possible OASPL is reached for the shortest duration noise, or in this case when the noise duration is 0.4 ms for an band-limited impulse focus. The plot further indicates that the OASPL reaches an asymptotic lower limit of ~92 dB for the longest durations above approximately 5s. The asymptotic lower limit could be due to the reverberation time of 7.6 seconds for the large reverberation chamber acting as a transient time building up to steady state. The

chamber is reaching a steady state of equal amounts of energy going into and out of the system. Thus, the amplitude shouldn't change once the steady state is reached. There's a difference of about 20 dB between the amplitude of a band-limited impulsive focus and the longest duration noise asymptote level, indicating the tradeoff of a reduced amplitude with a longer duration focus. It should be noted that the absolute OASPL values are specific to the equipment and settings used, but the relative differences in levels as a function of focused signal duration are helpful to be aware of.

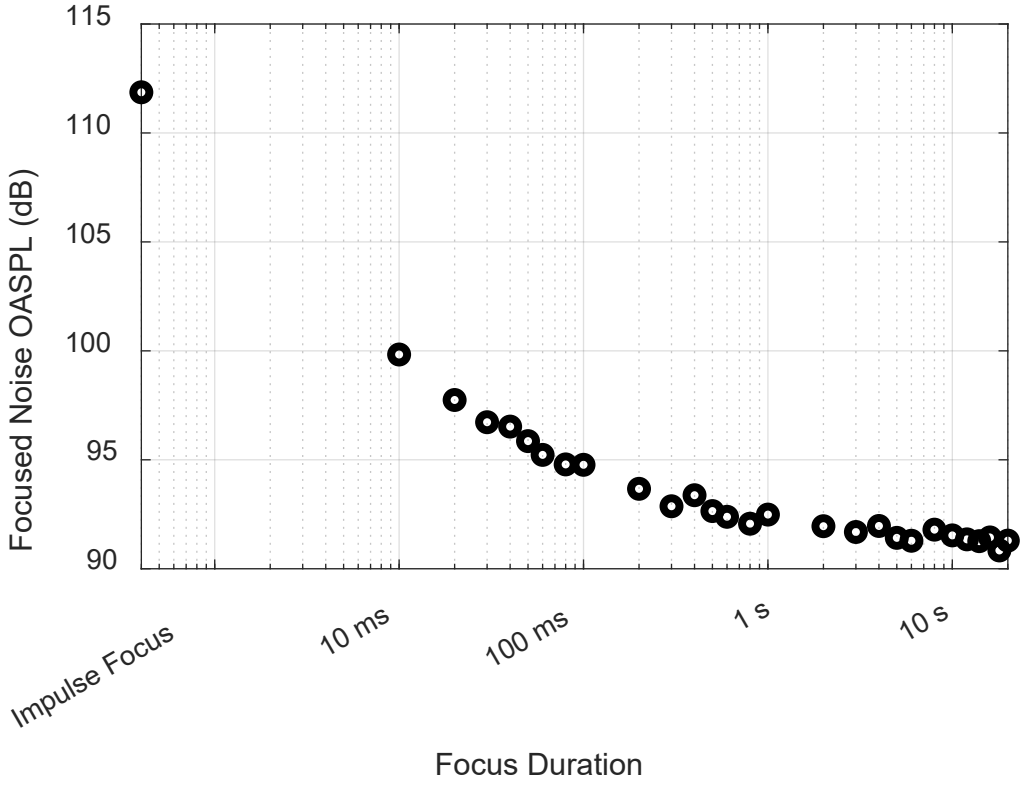

FIG. 2.5. Plot of the relationship between the duration of noise focused using time reversal vs. the overall sound pressure level (OASPL) of the steady state portion of the focused noise.

2.3.2 Coherent addition with increased number of sources

The next experiment will demonstrate that employing TR to focus identical noise signals leads to coherent amplitude addition when utilizing multiple loudspeakers simultaneously. These results will be directly compared to broadcasting the noise without using TR, highlighting a benefit of using TR. When the identical noise signals are convolved with the respective equalized TRIRs for each loudspeaker, TR provides a coherent transmission of the noise signal from all the loudspeakers to the microphone. In contrast, broadcasting identical noise signals (after one equalization step) without TR does not allow for coherent addition because the signal lacks the spatial encoding of the distance between the loudspeaker and the microphone and the room's reflection response, whereas the reversed impulse responses used in TR do contain this information.

In this experiment, equalized IRs from 8 loudspeakers to a fixed microphone location were obtained and convolved with the exact same noise signal (white noise in this case) for each loudspeaker. The bandwidth of the white noise is from 450 Hz (the lower frequency limit for the 500 Hz 1/3rd octave band) to 11.2 kHz (the upper frequency limit for the 1 kHz 1/3rd octave band) with a duration of 10 seconds. The analysis performed on this data was done with the steady state portion just like in Section 2.3.1. It's important to stress that the noise signals were not independently generated for each loudspeaker, it was truly the exact same noise signal. This same noise signal will also be broadcast without the use of TR for comparison.

Consistency in every input amplitude to each loudspeaker from ESTR was observed across all experiments, despite variations in the number of loudspeakers employed. The number of loudspeakers used increased by doubling, starting with one up to eight. While equalization was

applied during the experiments, it had no impact on the relative differences observed when different numbers of loudspeakers were used, nor on the relative differences between the results obtained for each method.

The benefits of TR start to appear when multiple loudspeakers are used. It is recommended to use as many loudspeakers as possible to see the largest gains when using TR. There is no significant difference between focusing the noise using TR and not focusing the noise when a single loudspeaker is used.

The results, given in Table 2.1, show that doubling the number of loudspeakers increases the OASPL by nearly 6 dB for each doubling of loudspeakers when focusing coherent noise signals. In contrast, Table 2.1 shows an OASPL increase of only 3 dB per doubling of loudspeakers when broadcasting equalized noise without TR. A 6 dB gain represents a coherent doubling of equal-amplitude sound pressure while a 3 dB gain represents an incoherent addition of equal-amplitude sound pressures. The average gains calculated in Table 2.1 deviate from the expected 3 dB or 6 dB increases due to variations in loudspeaker responses and loudspeaker locations, resulting in more or less efficient energy delivery.

If this TR experiment is conducted identically but instead of convolving the same noise signal with each of the different impulse responses, different noise signals (with non-identical phases) are used, the coherent addition that was previously occurring will no longer happen. This is because coherent addition relies on the phase alignment of the signals. When the phases are not identical, the constructive interference that leads to coherent addition is disrupted, resulting in a lower OASPL increase of 3 dB for a doubling of loudspeakers instead of 6 dB. Therefore, it is crucial to use the same identical noise source for each of the convolutions to obtain the coherent increase from TR.

TABLE 2.1. Comparison of overall sound pressure level (OASPL) values obtained under two conditions: (1) varying the number of loudspeakers with time reversal (TR) focusing of noise resulting in coherent addition of amplitudes, and (2) varying the number of loudspeakers while playing noise resulting in incoherent addition of amplitudes.

Number of Loudspeakers	Noise OASPL w/o TR (dB)	Gain (dB)	Noise OASPL w/ TR (dB)	Gain (dB)
1	78.9	N/A	78.7	N/A
2	82.7	3.8	85.2	6.5
4	85.5	2.8	90.4	5.2
8	89.1	3.6	97.0	6.6
	Average Gain	3.4		6.1

2.3.3 Desired spectral shape

The final study presented here illustrates how to focus noise with a desired spectral shape and the inherent tradeoffs encountered compared to focusing noise that is spectrally white. The MIL-STD-810G standard[34] specifies a spectral shape in relative levels at 1/3rd octave band frequencies and the use of 1/3rd octave bands in this standard is a motivating reason behind the specific inverse filter equalization and regularization process described previously in this paper. The equalization and regularization process described in Section 2.2.3. of broadcasting signals that consist of the noise convolved with the MIF TRIR will result in a spectrum at the focal location that has the same spectral shape as that of the noise signal used. The spectral shape of TR focusing results, when attempting to focus noise with various types of spectra, will be compared to the original spectral

shapes to ensure that the combination of equalization, regularization, and TR focusing proposed here indeed results in the desired spectral shape.

Various spectral shapes of band-limited noise to be focused include white noise, pink noise, and the MIL-STD-810G (METHOD 515.6 ANNEX A) standard noise. The standard spectrum analyzed alongside the white noise and pink noise is a test spectrum that is used for broadband random noise and incidence noise testing.[34] It is a standard that is used to test the integrity of structures or objects such as aircraft and rockets. Being able to recreate the acoustical environment with that spectrum is crucial for that type of testing on those structures. The data obtained here only utilized the 500 Hz-10 kHz 1/3rd octave bands to stay above the room's Schroeder frequency for all types of noise used, since exploring the use of the TR technique below a room's Schroeder frequency is beyond the scope of the current study. The MIL-STD-810G standard only specifies using noise up to the 10 kHz 1/3rd octave band hence our upper frequency limit. Different numbers of loudspeakers, denoted with different colors in the plots, were utilized to illustrate the relative increases in OASPL versus frequency as the number of loudspeakers was increased. The results presented in Fig. 2.6(a) demonstrate visually that focusing a white noise signal does indeed result in the spectral shape of white noise. It is noteworthy that the spectral shapes depicted in Fig. 2.6(a) closely align with those shown in Fig. 2.6(b), which involves broadcasting equalized white noise without utilizing TR. The coherent addition (~6 dB) that results from TR and the incoherent addition (~3 dB) that results from broadcasting random noise signals is also apparent in the spacing of the spectral results between the two images. Similarly, when examining the pink noise results in Fig. 2.6(c) and 2.6(d) and the military standard noise results in Fig. 2.6(e) and 2.6(f), identical trends are observed as in the case of white noise. This includes the resemblance in spectral shapes between TR and non-TR scenarios, alongside the higher OASPL observed in the TR case and the

benefits of coherent addition in the TR process. The dashed line with the circular markers represents the true spectral shape of white noise for Figs. 2.6(a) and 2.6(b), pink noise for Figs. 2.6(c) and 2.6(d), and the standard noise for Figs. 2.6(e) and 2.6(f). The true spectral shape absolute levels are arbitrary fitted to the trial involving the highest number of loudspeakers to provide a good visual comparison. These results demonstrate that TR can be used to focus noise with a specific spectral shape of interest.

When using different types of noise, there are tradeoffs to consider. The OASPL of an 8-loudspeaker broadcast for focusing white noise is 97.0 dB. In comparison, pink noise under the same conditions has an OASPL of 99.8 dB, and the standard noise has an OASPL of 104.0 dB. The gain in OASPL depends on the frequency content of the chosen noise and the frequency dependence of the reverberation time in the room used. Pink noise and the standard noise, which relatively contain more low-frequency energy than white noise, result in a higher OASPL because lower frequencies are more efficient for TR transmission due to the longer reverberation times at lower frequencies in this reverberation chamber.

The results are plotted on a logarithmic frequency axis, which is important to note for understanding the spectra of white noise and pink noise. White noise is characterized by having equal energy per frequency, meaning that as the frequency increases, each 1/3rd octave band contains more energy due to the widening of the band. However, because the x-axis is logarithmic, this does not result in a flat line but an increasing trend. On the other hand, pink noise has equal energy per octave, meaning the energy in each octave band is constant regardless of the frequency. Since the x-axis is logarithmic and each octave covers more frequencies as frequency is increased,

pink noise results in a flat line with a logarithmic frequency axis. As before, the calculation of the 1/3rd octave band levels only utilized the steady state portion of the time signal when calculating OASPL.

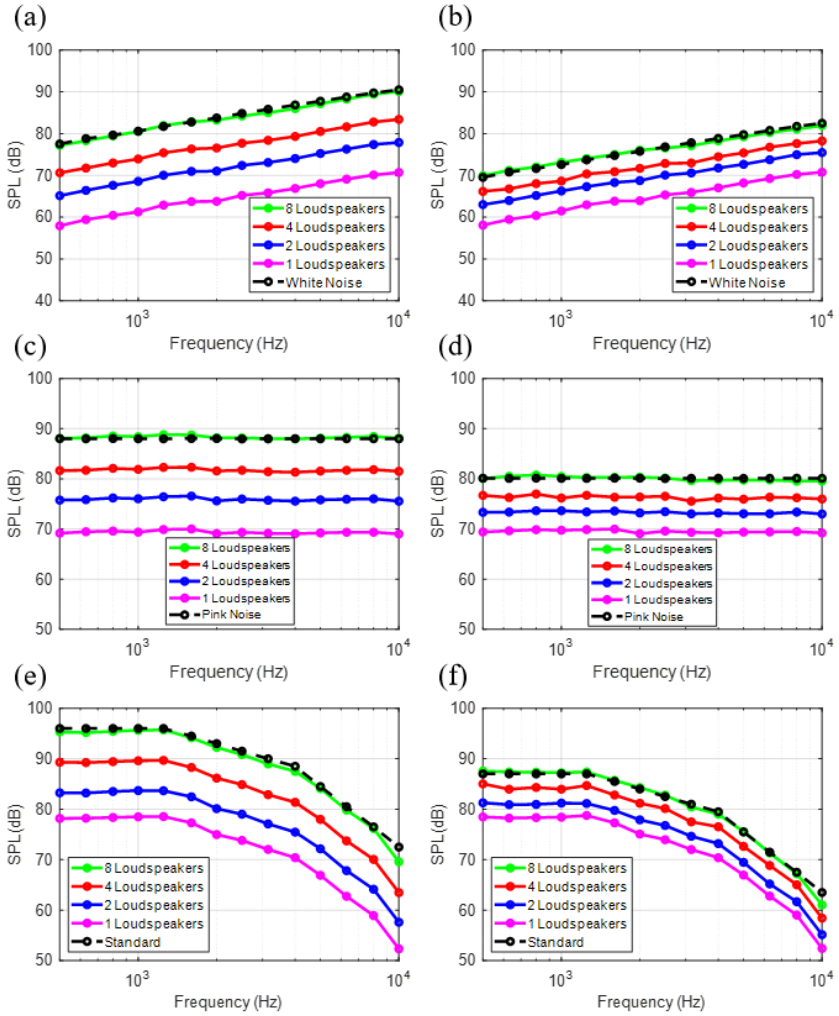

FIG. 2.6. The comparison of spectral shapes depicts (a) white noise with TR, (b) white noise without TR, (c) pink noise with TR, (d) pink noise without TR, (e) military standard noise with TR, and (f) military standard noise without TR scenarios utilizing varying numbers of loudspeakers (solid lines). The dashed black line with the circular markers represents the true spectral shape of the noise, whose amplitude is fitted to the trial involving the highest number of loudspeakers.

2.4 Conclusion

The results presented in this paper explore issues encountered when using TR to focus noise signals. It was demonstrated that the duration of focusing affected the OASPL. The longer the duration of the focused noise, the lower the OASPL that resulted and vice versa, but when the duration exceeded 5 s, a lower bound asymptotic value of 20 dB less than the focused impulse amplitude was reached. It was also found that using TR to focus identical, synchronized noise signals compared to broadcasting identical, synchronized noise signals without TR resulted coherent addition of ~6 dB in OASPL with TR when using double the number of loudspeakers, compared to a ~3 dB increase observed without TR. This is due to the coherence inherent in the constructive interference created by the TR process when focusing with multiple loudspeakers. Lastly, focusing noise with a desired spectral shape, with proper equalization, was explored using TR. The results again showed the coherent addition benefits of using TR with multiple loudspeakers, and tradeoffs were observed when focusing noise of various spectral shapes. These tradeoffs consist of the changing of the OASPL, with differences in frequency content (due to factors like a frequency dependent reverberation time) leading to variations in OASPL.

2.5 References

[1] M. Fink, "Time reversed acoustics," *Phys. Today* **50**(3), 34-40 (1997).

[2] B. E. Anderson, M. Griffa, C. Larmat, T.J. Ulrich, and P.A. Johnson, "Time reversal," *Acoust. Today* **4**(1), 5–16 (2008).

[3] C. S. Clay and B. E. Anderson, "Matched signals: The beginnings of time reversal," *Proc. Meet. Acoust.* **12**(1), 055001 (2011).

[4] J. V. Candy, A. W. Meyer, A. J. Poggio, and B. L. Guidry, "Time reversal processing for an acoustic communications experiment in a highly reverberant environment," *J. Acoust. Soc. Am.* **115**(4), 1621–1631 (2004).

[5] J. V. Candy, D. H. Chambers, C. L. Robbins, B. L. Guidry, A. J. Poggio, F. Dowla, and C. A. Hertzog, "Wideband multichannel time-reversal processing for acoustic communications in highly reverberant environments," *J. Acoust. Soc. Am.* **120**(2), 838–851 (2006).

[6] M. Fink, G. Montaldo, and M. Tanter, "Time-reversal acoustics in biomedical engineering," *Annu. Rev. Biomed. Eng.* **5**, 465–497 (2003).

[7] S. M. Young, B. E. Anderson, S. M. Hogg, P.-Y. L. Bas, and M. C. Remillieux, "Nonlinearity from stress corrosion cracking as a function of chloride exposure time using the time reversed elastic nonlinearity diagnostic," *J. Acoust. Soc. Am.* **145**(1), 382–391 (2019).

[8] B. E. Anderson, M. C. Remillieux, P.-Y. Le Bas, and T. J. Ulrich, "Time reversal techniques," in Nonlinear Acoustic Techniques for Nondestructive Evaluation, 1st ed., edited by T. Kundu (Springer and Acoustical Society of America, New York, 2018), pp. 547–581.

[9] C. Larmat, J.-P. Montagner, M. Fink, Y. Capdeville, A. Tourin, and E. Clevede, "Time-reversal imaging of seismic sources and applications to the great Sumatra earthquake," *Geophys. Res. Lett.* **33**(19), L19312, (2006).

[10] A. Sutin, A. Sarvazyan, P. A. Johnson, and J. A. TenCate, "Land mine detection by time-reversal acousto-seismic method," *J. Acoust. Soc. Am.* **115**(5), 2384(A) (2004).

[11] G. Ribay, J. de Rosny, and M. Fink, "Time reversal of noise sources in a reverberation room," *J. Acoust. Soc. Am.* **117**(5), 2866-2872 (2005).

[12] B. E. Anderson, M. Clemens, and M. L. Willardson, "The effect of transducer directionality on time reversal focusing," *J. Acoust. Soc. Am.* **142**(1), EL95–EL101 (2017).

[13] B. Van Damme, K. Van Den Abeele, Y. Li, and O. Bou Matar, "Time reversed acoustics techniques for elastic imaging in reverberant and nonreverberant media: An experimental study of the chaotic cavity transducer concept," *J. Appl. Phys.* **109**, 104910 (2011).

[14] M. Tanter, J. Thomas, and M. Fink, "Time reversal and the inverse filter," *J. Acoust. Soc. Am.* **108**(1), 223–234 (2000).

[15] M. H. Denison and B. E. Anderson, "Time reversal acoustics applied to rooms of various reverberation times," *J. Acoust. Soc. Am.* **144**, 3055-3066 (2018).

[16] T. S. Furlong, B. E. Anderson, B. D. Patchett, and S. D. Sommerfeldt, "Active noise control using remotely placed sources: Application to magnetic resonance imaging noise and equivalence to the time reversal inverse filter," *Appl. Acoust.* **176**, 107902 (2021).

[17] S. Yon, M. Tanter, and M. Fink, "Sound focusing in rooms: The time-reversal approach," *J. Acoust. Soc. Am.* **113**(3), 1533–1543 (2003).

[18] M. L. Willardson, B. E. Anderson, S. M. Young, M. H. Denison, and B. D. Patchett, "Time reversal focusing of high amplitude sound in a reverberation chamber," *J. Acoust. Soc. Am.* **143**(2), 696-705 (2018).

[19] B. D. Patchett and B. E. Anderson, "Nonlinear characteristics of high amplitude focusing using time reversal in a reverberation chamber," *J. Acoust. Soc. Am.* **151**(6), 3603-3614 (2022).

[20] B. D. Patchett, B. E. Anderson, and A. D. Kingsley, "The impact of room location on time reversal focusing amplitudes," *J. Acoust. Soc. Am.* **150**(2), 1424-1433 (2021).

[21] B. D. Patchett, B. E. Anderson, and A. D. Kingsley, "Numerical modeling of Mach-stem formation in high-amplitude time-reversal focusing," *J. Acoust. Soc. Am.* **153**(5), 2724-2732 (2023).

[22] C. B. Wallace and B. E. Anderson, "High-amplitude time reversal focusing of airborne ultrasound to generate a focused nonlinear difference frequency," *J. Acoust. Soc. Am.* **150**(2), 1411-1423 (2021).

[23] T. J. Ulrich, B.E. Anderson, P.Y. Le Bas, C. Payan, J. Douma, and R. Snieder, "Improving time reversal focusing through deconvolution: 20 questions," *Proc. Meet. Acoust.* **16**, 045015 (2012).

[24] B. E. Anderson, J. Douma, T. J. Ulrich, and R. Snieder, "Improving spatio-temporal focusing and source reconstruction through deconvolution," *Wave Mot.* **52**, 151-159 (2015).

[25] G. Montaldo, M. Tanter, and M. Fink, "Real time inverse filter focusing through iterative time reversal," *J. Acoust. Soc. Am.* **115,** 768–775 (2004).

[26] P.-Y. Le Bas, T. J. Ulrich, B. E. Anderson, and J. J. Esplin, "A high amplitude, time reversal acoustic non-contact excitation," *J. Acoust. Soc. Am.* **134**(1), EL52-EL56 (2013).

[27] P.-Y. Le Bas, M. C. Remillieux, L. Pieczonka, J. A. Ten Cate, B. E. Anderson, and T. J. Ulrich, "Damage imaging in a laminated composite plate using an air-coupled time reversal mirror," *Appl. Phys. Lett.* **107**, 184102 (2015).

[28] M. Farin, C. Prada, and J. de Rosny, "Selective remote excitation of complex structures using time reversal in audible frequency range," *J. Acoust. Soc. Am.* **146**, 2510-2521 (2019).

[29] M. Farin, C. Prada, T. Lhommeau, M. El Badaoui, and J. de Rosny, "Towards a remote inspection of jet engine blades using time reversal," *J. Sound Vib.* **525**, 116781 (2022).

[30] B. E. Anderson, R. A. Guyer, T. J. Ulrich, and P. A. Johnson, "Time reversal of continuous wave, steady-state signals in elastic media," *Appl. Phys. Lett.* **94**(11), 111908 (2009).

[31] M. R. Schroeder, "The 'Schroeder frequency' revisited," *J. Acoust. Soc Am.* **99**(5), 3240–3241 (1996).

[32] ISO 3741:2010, "Sound power and energy in reverberant environments" (International Organization for Standardization, Geneva, Switzerland, 2010).

[33] A. D. Kingsley, J. M. Clift, B. E. Anderson, J. E. Ellsworth, T. J. Ulrich, and P.-Y. Le Bas, "Development of software for performing acoustic time reversal with multiple inputs and outputs," *Proc. Meet. Acoust.* **46**, 055003 (2022).

[34] "MIL-STD-810G" (Department of Defense Test Method Standard, 515.6A-4 (2008))

Chapter 3

Optimizing the spatial extent of long duration broadband noise signals using time reversal

The use of audible sound for acoustic excitation is commonly employed to assess and monitor structural health, as well as to replicate the acoustic environmental conditions that a structure might experience in use. Achieving the required amplitude and specified spectral shape is essential to meet industry standards. This study aims to implement a sound focusing method called time reversal (TR) to achieve higher amplitude levels compared to simply broadcasting noise. The paper seeks to understand the spatial dependence of focusing long-duration noise signals using TR to increase the spatial extent of the focus. Both one- and two-dimensional measurements are performed and analyzed using TR with noise, alongside traditional noise broadcasting without TR. The variables explored include the density of foci for a given length/area, the density of foci for varying length with a fixed number of foci, and the frequency content and bandwidth of the noise. A use case scenario is presented that utilizes a single-point focus with an upper frequency limit to maintain the desired spectral shape while achieving higher focusing amplitudes.

3.1 Introduction

Time reversal (TR) is a method most commonly used to focus impulsive-like sounds.[1,2] Some applications that use impulsive TR include biomedical ultrasound,[1,3] communication in various media,[1,4,5,6,7] and nondestructive evaluation.[1,8,9] However, TR is not limited solely to focusing impulsive sounds. TR has been shown to effectively focus single frequency tones,[10, 11] short duration noise,[12] and long duration noise (described in Chapter 2). An application of focusing long-duration noise signals is using TR to locate non-volcanic tremor.[13] The current paper continues the study of focusing long duration noise signals, but more specifically the spatial extent of this focusing.

Focusing long-duration noise signals follows a similar process to that of impulsive-like signals but includes an additional step. Both methods begin by obtaining an impulse response (IR). A loudspeaker placed in a room broadcasts a swept sine wave (chirp), and the response of this chirp, known as the chirp response (CR), is recorded at a location where focusing is desired that is determined by the placement of a microphone within the room. The IR is calculated using a cross-correlation method.[14] For the cross-correlation method to yield an IR with accurate timing, when using multiple channels for TR, the broadcasted and recorded signals need to be time-synced. It is important to note that moving the loudspeaker to a different location after calculating the IR will prevent the sound waves from focusing at the original microphone location. The process up to this point will be known as the forward step. The remaining process is referred to as the backward step. Reversing the impulse response generates a time-reversed impulse response (TRIR). For impulsive focusing, broadcasting the TRIR from the same loudspeaker results in an impulsive-like focusing at the microphone. For focusing long-duration noise, an extra step is required: the TRIR is

convolved with the noise signal prior to its broadcast. Broadcasting the convolved signal enables long-duration focusing through constructive interference between the direct sound waves and their reflections. The use of additional loudspeakers in TR provides even higher amplitude focusing.

Certain previous studies on impulsive focusing of audible sound in rooms are considered especially relevant to the research conducted in a reverberation chamber in this paper, despite differences in their primary application. Yon *et al.*[15] showed that increasing the bandwidth and/or number of sources created a higher quality (more prominent) peak compared to the spatial sidelobes of the TR focusing. Candy *et al.*[4] demonstrated that TR transducers can effectively operate in highly reverberant environments, detecting and recovering transmitted information with zero errors. Denison *et al.*[16] concluded that decreasing the volume and absorption of a room increases the focal amplitude and quality of the focusing. Some researchers have explored high amplitude focusing of sound in rooms and the nonlinear properties of that focusing.[17,18] Farin *et al.*[19,20] explored TR focusing of sound to excite complex structures, enabling selective excitation and damage detection without disassembly.

A study by Ribay *et al.*[12] explored the focusing of pulses and short-duration noise signals. It was found that the quality of the focusing increased as the number of loudspeakers increased. Anderson *et al.*[10] found that multiple sources must be used to obtain TR spatial focusing of single-frequency tones. In Chapter 2 the focusing of long-duration noise with a desired spectrum at a single location was shown, achieving increased amplitude compared to merely broadcasting the noise. Ribay *et al.*,[12] Anderson *et al*.,[10] and Chapter 2 each demonstrated the concept of coherent addition in their respective contributions.

Previous studies explored the spatial extent of impulsive focusing. Tanter *et al.*[21] showed that applying an inverse filter in TR focusing can reduce spatial sidelobes amplitudes. Others have also

explored TR with the use of an inverse filter/deconvolution.[22,23] Yon *et al.*[15] found that increasing the number of loudspeakers used for TR focusing decreases the focus spot diameter and the relative amplitude of spatial sidelobes in free space, but that in a reverberation chamber the spot diameter depends more on the center frequency than the number of loudspeakers. Kingsley *et al.*[24] explored the spatial extent of multipoint focusing with different spatially shaped foci. By applying a spatial inverse filter they were able to achieve dipole, quadrupoles and "Y" shaped patterns.

Anderson *et al*.[25] conducted a study on the spatial reconstruction of pulses with a center frequency of 200 kHz using TR techniques with ultrasonic elastic waves in an aluminum plate. The experiments utilized virtual sources, starting with two foci and increasing up to 25 foci, with a constant 1 mm spacing between each source. The objective was to simulate sources spanning from a point source up to an extended line source spanning a linear distance of 1.5 wavelengths. The study evaluated several metrics: the peak magnitude of the TR focus, the ratio of the peak magnitude to the next highest spatial peak, the comparison of peak magnitude to the average wave field magnitude (excluding the main focal lobe), and the ratio of peak focal magnitude to the highest temporal side lobe magnitude. The findings indicated that the ability to spatially reconstruct coherent sources with TR foci diminishes as the source size exceeds half a wavelength.

This paper extends the study of focusing broadband audible noise, specifically examining the spatial extent of the focus under various conditions. The purpose of this paper is to quantify how the spatial extent of TR focusing (with a single focus or multiple foci) depends on factors such as the density of focus points for a given length/area of focusing, the variation in length of focusing with a fixed number of focus points, and the frequency content and bandwidth of the noise. The study found that adjusting the density of focus locations affects both the overall sound pressure level (OASPL) and the shape of the desired spectrum, whether the density of foci was explored in

one or two dimensions. Constructive and destructive interference was observed most prominently between adjacent focus points, depending on their spacing and frequency. By applying an equalization step, the spectra were corrected, revealing an upper frequency limit for focusing a desired frequency bandwidth across various target areas. This method produced higher spatially averaged amplitude compared to broadcasting noise signals, offering a practical solution for achieving higher amplitude gains without distorting the spectral shape.

3.2 Experimental setup

3.2.1 Setup

Spatial measurements of sound fields were measured using a 2D scanning system at Brigham Young University. The scanning system has two controllers (Applied Motion Products STAC 6i) that connect to stepper motors (Applied Motion Products HT23-550D) that control the position of a microphone that extends away from the system on a small pole. The scanning system can move the microphone in a plane, in a 2 x 2 m^2 area. The scanning system is operated through a custom LabVIEW™ program called Easy Spectrum Time Reversal (ESTR)[26]. ESTR offers various functions for facilitating TR experiments. It integrates with Spectrum M2i.6022 and M2i.4931 signal generation and digitizer cards, enabling synchronized broadcasting and recording. This synchronization is crucial for ensuring that TRIR broadcasts from multiple loudspeakers reach the focus location simultaneously to ensure precise timing.

ESTR can broadcast and record signals for each loudspeaker either simultaneously or sequentially at each scanning grid position with the 2D scanning system, which is set to pause at each location when recording before proceeding to the next location. This automation of the forward and backward steps is essential, particularly when the number of microphones is limited, as it allows for experiments to be conducted across multiple recording locations for a repeatable experiment in a timely manner. For the experiment to be repeatable it is assumed the conditions of the room are not changing, such as temperature. There are some prepping steps in between the forward step and backward step for focusing long duration noise signals discussed in Section 3.2.2.

The reverberation chamber has dimensions of 4.96 m × 5.89 m × 6.98 m (volume of 204 m^3). The Schroeder frequency of the chamber is 410 Hz with a reverberation time of 7.6 s.[18,27] However, the lowest frequency used across all signals in the experiments is 56 Hz, corresponding to the lowest frequency in the 63 Hz 1/3rd octave band. Diffuser panels hang from the ceiling of the chamber, which serve to randomize the propagation directions of reflections in the sound field. To achieve higher focal amplitudes Mackie HR824mk2 loudspeakers, placed on stands about 1 m off of the floor, were each placed facing the nearest wall about 15 cm away. This orientation was chosen to minimize the direct sound amplitude.[14] The microphone used in all experiments was a G.R.A.S. 46AQ 1.27 cm (0.5 inch) pre-polarized, random-incidence microphone, which was mounted on the arm of the 2D scanning system and powered by a G.R.A.S 12AX signal conditioner. To adhere to standards for being in the diffuse field[28] and to prevent a doubling of pressure,[29] the microphone was always positioned at least 1 m away from any wall or large surface. Since the 2D plane was oriented vertically in the room (as shown in Fig. 3.1), the scanning grid was set to ensure it remained 1 m above the ground.

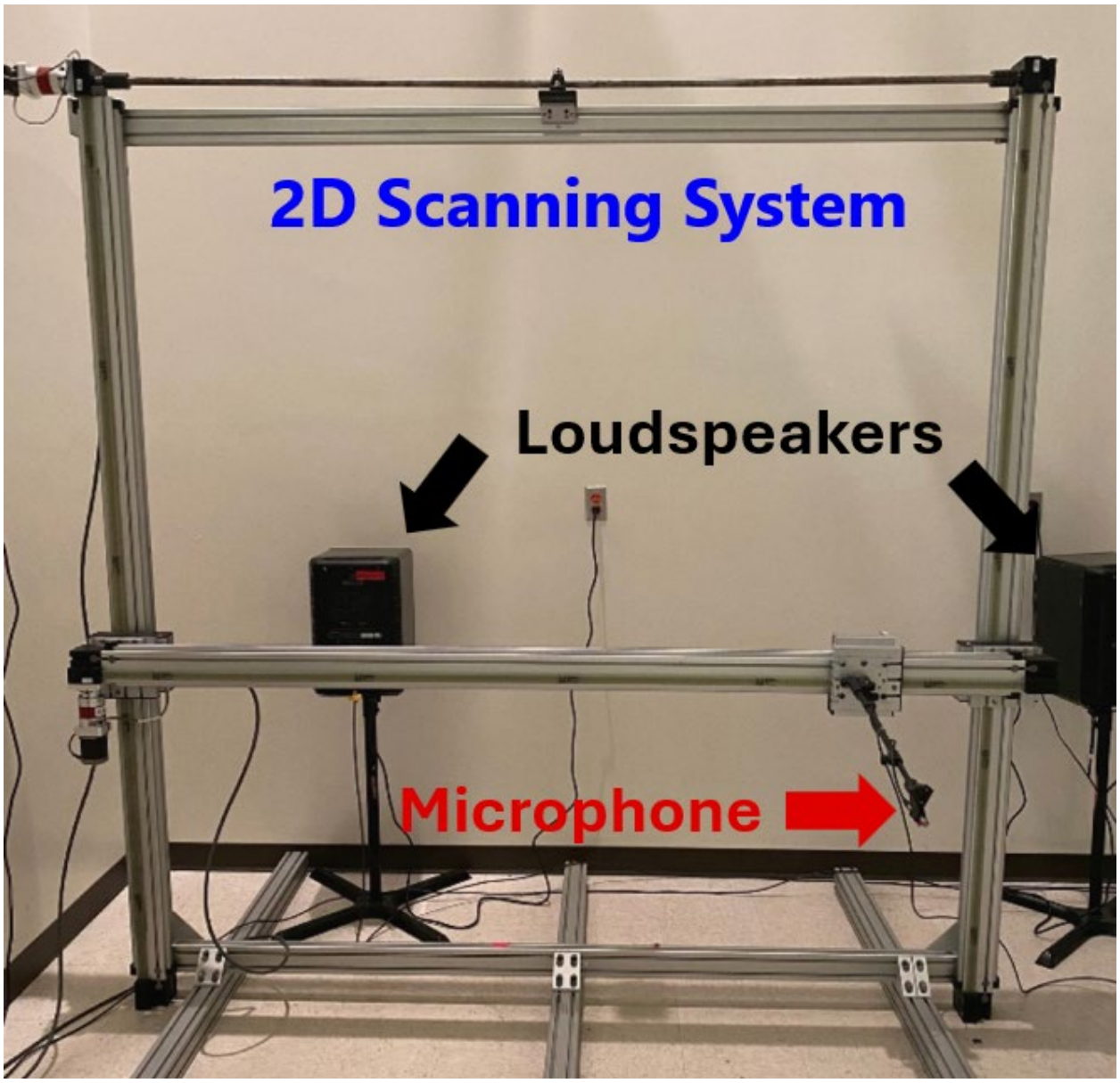

FIG. 3.1. Photograph of loudspeakers (black arrows) and a microphone (red arrow) mounted to the arm of the 2D scanning system placed in the reverberation chamber at Brigham Young University.

3.2.2 Multipoint time reversal focusing

To explore increasing the spatial extent, focusing to multiple locations will be done simultaneously. For simplicity and clarity, consider the following thought experiment with two focus locations and two loudspeakers.

The process of focusing to multiple locations begins by gathering IRs, as described in Section 3.1. In this case, IRs are collected from each loudspeaker to each focal location, resulting in a total of four IRs—two IRs from each loudspeaker to the two focal points. These IRs contain the necessary timing information of sound arrivals to create a focus at each desired location. To create multiple foci, each IR, $h(t)$, is reversed in time to obtain the TRIR, $h(-t)$.

For focusing broadband noise, we first convolve the noise signal $n(t)$ with each TRIR $h(-t)$,

$$cs(t) = h(-t) * n(t). \tag{3.1}$$

Each convolved signal, $cs(t)$, corresponds to the signal used to focus noise at a specific location when broadcast. The next step involves broadcasting these convolved signals, which is equivalent to convolving with the original IRs, resulting in focused noise signals, $f_n(t)$, at each location,

$$f_n(t) = cs(t) * h(t). \tag{3.2}$$

The $f_n(t)$ signals generated by each loudspeaker superpose constructively at the focal location. To achieve this, the $cs(t)$ signals used to focus at each focal location are added together prior to their broadcast to produce a combined signal that will be broadcast from each respective loudspeaker. It is important to note that for the signals to sum correctly, the individual signals need to be time synchronized. This ensures that focusing at both locations is done simultaneously by both loudspeakers. This approach may be generalized to any number of loudspeakers and any number of desired focal points.

3.2.3 Equalization process of broadcasted signals

Equalizing a convolved signal before broadcasting is crucial for achieving the desired spectrum at the focal location(s). The purpose for equalizing is to compensate for an uneven frequency response of the loudspeakers, a spatially averaged variation in gain from room modes over frequency, and frequency-dependent absorption effects during propagation. Equalization is performed in the frequency domain by taking the Fast Fourier Transform of the IR to obtain the transfer function, separating it into magnitude and phase components, and then modifying the magnitude while preserving the phase.

The inverse filter process addresses the magnitude disparity between the desired spectrum and the one distorted by propagation through the room twice (propagation during the forward and backward steps of TR). The Half Inverse Filter (HIF) spectrum is used to equalize the signal to compensate for the uneven frequency response during a single broadcast step. The HIF is calculated by dividing the chirp spectrum by the CR spectrum. Regularization is applied to the magnitude of the HIF spectrum to reduce high amplitudes in the HIF at inefficient transmitting frequencies, which helps avoid inefficiencies in transmission. This is achieved by dividing the HIF spectrum into 1/3rd octave bandwidths, calculating the median amplitude for each bandwidth, and setting the amplitude of any frequencies that exceed this median equal to the median value. Tanter *et al.*[21] used single value decomposition (SVD) to minimize large errors from small systemic errors during inversion. Similarly, Anderson *et al.*[23] applied regularization by adding a finite value to the inverse filter denominator, reducing background noise by preventing division by zero or small

values outside the bandwidth. However, this issue of amplifying noise outside of the bandwidth is not a problem with the implementation used here because the inverse filter is applied only to the frequencies being used. The frequencies are modified only within each 1/3rd octave band, not across the overall spectrum.

Regularization applied to the HIF spectrum results in a signal that is not dominated by frequencies that were weakly received during the forward step and thus amplified the most by a HIF without regularization. This leads to a more efficient broadcast of overall energy. To achieve a TR focal signal that has a flat spectrum, the HIF must be applied to the $cs(t)$ twice to compensate for the forward step propagation that has already happened and to anticipate the frequency dependence of the backward step propagation. To generate equalized noise at a location without the use of TR, the HIF is only applied once in anticipation of the single propagation step. The phase of the $cs(t)$ spectrum or noise spectrum is reattached after the HIF multiplications and regularization prior to performing an inverse Fast Fourier Transform to obtain the time domain signal to be broadcast. It is important to note that the chosen noise signal convolved with the TRIR may have any desired spectrum. For additional details on this methodology and implementation, please refer to Section 2.2.3.

3.3 Experimental results

3.3.1 One-dimensional scans

One-dimensional multipoint focusing is now discussed. The scanning system moved horizontally without any vertical movement. All data were obtained exclusively through experimental measurements for both the forward and backward steps. The sound pressure levels are given in dB relative to $20\,\mu Pa$. The two primary experiments for one-dimensional scans explore varying the following two parameters: the density of foci within a fixed length (progressively adding more and more individual foci) and the density of foci across different lengths with a fixed number of foci (progressively spreading out the distance between all adjacent foci). White noise was used in these experiments with frequency content between the 630 Hz and 10 kHz 1/3rd octave bands. The plots presented have position and frequency on the x-y plane, with amplitude measured in dB on the z axis. The frequency information displayed in the plots are not narrowband, but rather 1/3rd octave band levels. Plotted in this way, white noise exhibits a linearly increasing trend with increasing frequency because each 1/3rd octave band represents more energy at higher frequencies, whereas, for example, pink noise would appear as a flat line due to its equal energy distribution per octave.

For reference, Fig. 3.2(a) shows the results of a 1D scan of non-focused noise present at those locations that was equalized to produce a white noise spectrum. In contrast, Fig. 3.2(b) presents a scan of the field at those locations with a single point TR focus at the 0.75 m mark using equalized white noise. The previous study in Chapter 2 indicated that at the focus location, both focused and

non-focused noise maintain the same noise spectra, with the focused noise having a higher amplitude of roughly 3 dB gain per doubling of loudspeakers. This pattern is evident in the comparison of Figs. 3.2(a) and 3.2(b) at the focus location, though the single point focus exhibits an expected spatial width that varies with frequency. Locations away from the focus location thus have lower amplitude at all frequencies. While the increased amplitude from using TR is advantageous, the spatial extent of the focus is limited to a wavelength in size with a single focus location. However, by focusing at multiple locations, the spatial extent of the focused noise might be extended, thereby increasing the amplitude gain from TR over a larger region.

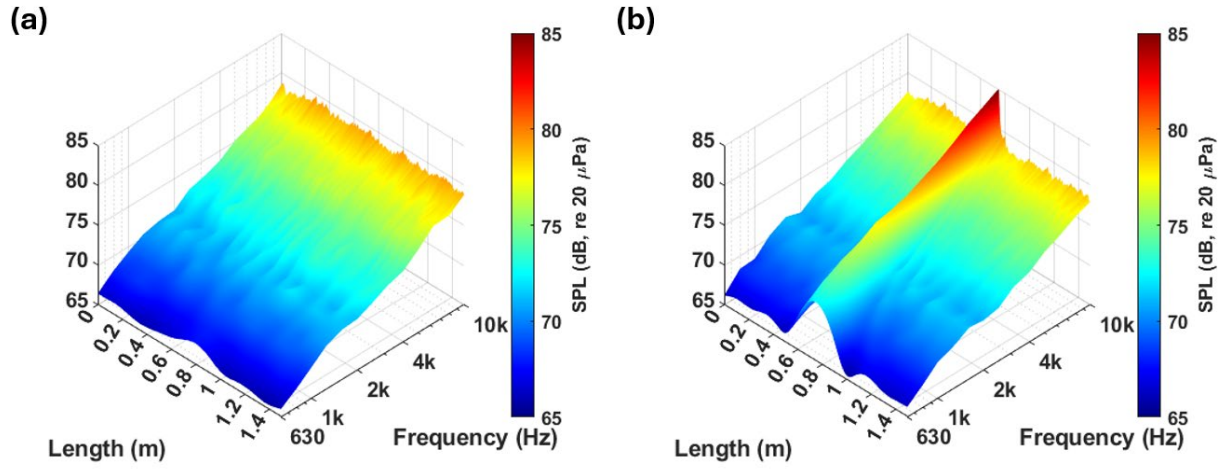

FIG. 3.2. One-dimensional spatial scan of broadcasting a) equalized noise to achieve a white noise spectrum everywhere in the reverberation chamber, b) focusing equalized noise to achieve a white noise spectrum at the focus location.

In the first study, the density of multiple, simultaneous TR foci was varied within a fixed span length of 1.28 m, referred to as the target region, where the focal locations were limited to. To observe edge effects from the focus locations situated at the farthest left and right positions, the total scan length was extended to 1.5 m. Measurements were made every 1 cm across the scan line.

The number of foci created were as follows: 1, 4, 5, 9, 17, 33, 65, and 129, all focused within the target region with equal spacing between adjacent foci.

Figure 3.3 shows the OASPL as a function of position along the scan line. The results indicate that it is possible to focus long-duration noise signals at multiple locations with higher amplitude than without TR focusing. Lower densities of focal locations result in more distinctive focal hot spots across the target region, which is not ideal when a spatially uniform distribution of noise is desired. As the density of foci increases, the OASPL levels become more spatially uniform across the target region and larger in amplitude, compared to the pronounced spikes observed with lower numbers of foci. This spatial uniformity in OASPL and increased overall amplitude are benefits of using TR with noise, but a deeper analysis reveals that it may not be ideal in terms of frequency content. It is worth noting that when comparing the 65 and 129 foci results, there appears to be a saturation density of points within a given length, which does not result in additional amplitude gains. Based on this data, for the given target region and frequency content, the optimal focal density appears to lie somewhere between 33 and 65 focal locations. This observation was not explored further beyond what is noted here. As for the no focusing case, the random spikes occur due to the combined contribution of room modes at each location, where certain areas experience greater constructive interference.

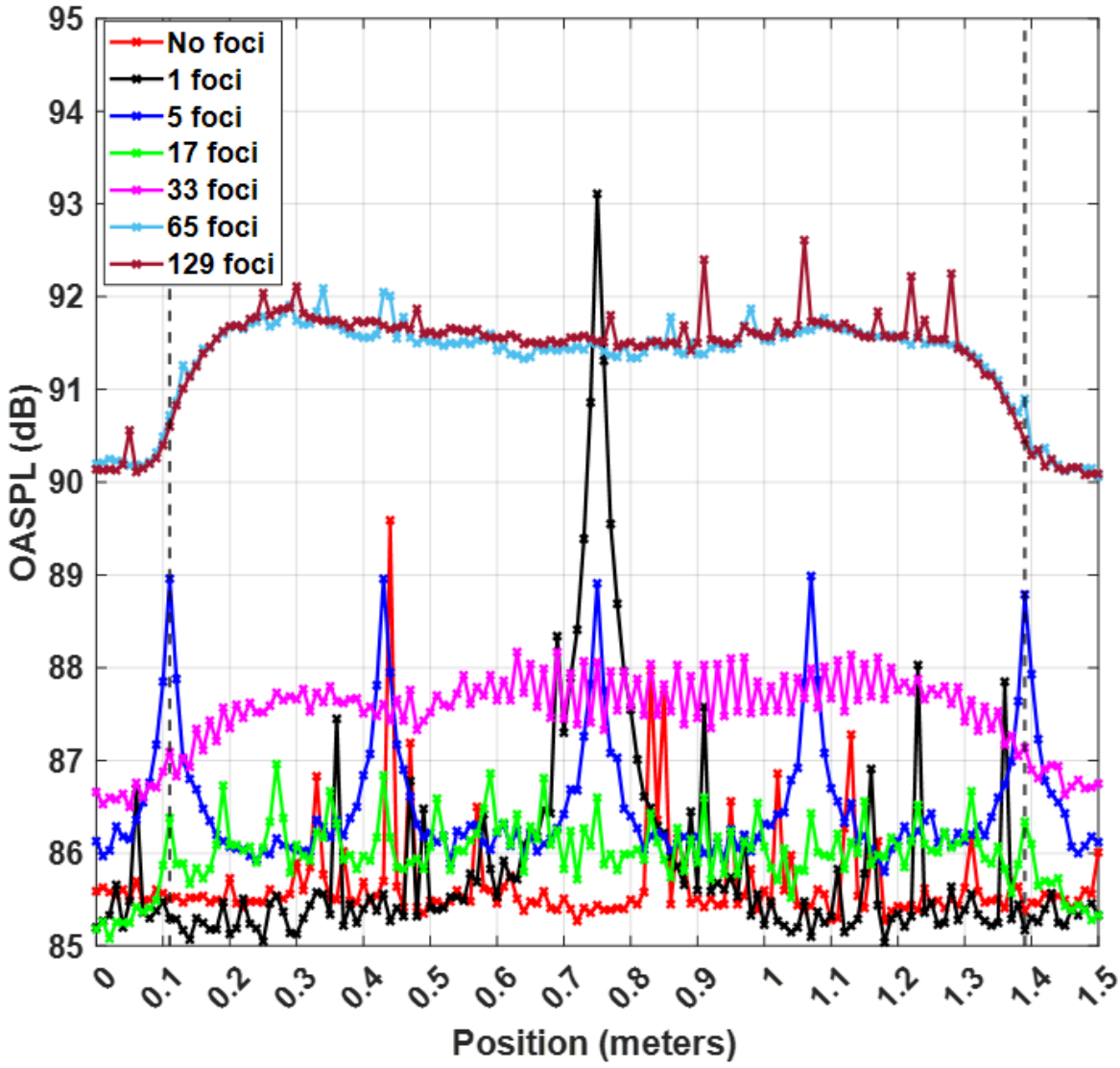

FIG. 3.3. Overall sound pressure level (OASPL) as a function of position when varying numbers of TR foci are generated. Black vertical lines represent the 1.28-meter length of which the foci are confined to.

Figure 3.4 presents the results for 5, 17, 33, and 129 simultaneous focal locations as a function of position, frequency, and level. A video link is provided in Mm. 1 to show the progression in these plots as the number of focal locations in increased, including results not shown in Fig. 3.4.

Observing the plots in Fig. 3.4, it is apparent that the different densities of focus locations affect the spectral shape. The desired spectral shape should resemble the slope in Fig. 3.2(a) of +3 dB/octave. This does happen for the spectra at lower focal densities, such as in Fig. 3.4(a). The individual ridges in Fig. 3.4(a) closely resemble the slope of the ridge in Fig. 3.2(b), but with a smaller amplitude increase for the 5 focus location ridges. Obtaining the desired spectrum of the noise is a critical desired outcome, but the spatial uniformity still remains a problem with only 5 foci. As the density of foci increases, the OASPL is more spatially uniform, as seen in Fig. 3.3, but higher density foci also results in spectra that depart from the spectrum of white noise.

Mm. 1. An animation of the progression as the number of focal locations increasing from 4, 5, 9, 17, 33, 65, and 129, showing plots of amplitudes as a function of space and frequency. This is a file of type ".mp4" https://youtu.be/SLgFWhcjdpI (0.092 MB).

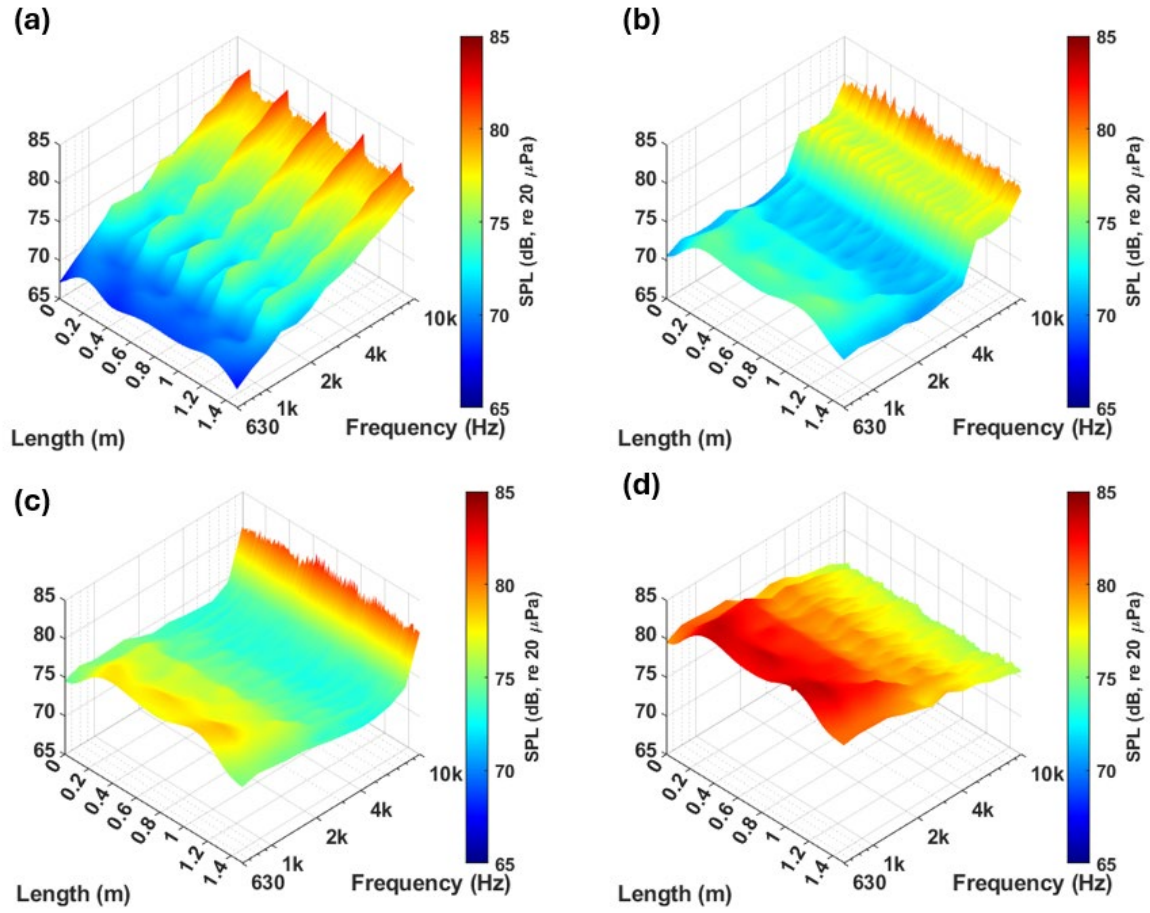

FIG. 3.4. Sound pressure level as a function of space and frequency (1/3rd octave band levels are plotted). The number of time reversal foci is varied while the span of the foci is kept the same: a) 5, b) 17, c) 33, and d) 129 foci.

Analyzing Fig. 3.4, there is a noticeable dip in the 1/3rd octave band levels over a small range of frequency as the density of the foci increases. The dip occurs at a frequency whose wavelength is similar to the spacing between the foci. For example, in the case of 17 foci (Fig. 3.4(b)), the spacing between foci is 8 cm, and if this distance were a wavelength it would correspond to a frequency of approximately 4.3 kHz and fall within the 4 kHz 1/3rd octave band, where the

amplitude dips. As the spacing between the foci decreases, the corresponding frequency of the dip increases. In Fig. 3.4(c), where the foci are spaced 4 cm apart, a wavelength of this distance would correspond to a frequency of approximately 8.6 kHz falling within the 8 kHz 1/3rd octave band, again approximately where the dip in amplitude is observed.

This dip can be explained with the use of a finding of Cassereau and Fink[30] who used the Cardinal sine, or $\mathrm{sinc}(kx) = \sin(kx)/kx$, function to model the optimal spatial extent of time-reversal focusing of waves in spherical coordinates, where k is the wavenumber. The authors of the current paper verified that the spatial dependence of the focusing in all 3 dimensions is in fact a $\mathrm{sinc}(kx)$ function by placing hundreds of point sources at various angles surrounding an origin with equal radial distances. A single frequency sine wave was simultaneously broadcast from all of these sources and the resultant interference near the origin was observed to in fact be a $\mathrm{sinc}(kx)$ function in any dimension. For the TR focusing to result in a $\mathrm{sinc}(kx)$ function, waves need to converge from all directions of approximately equal amplitude, and this is mostly likely to happen in a highly reverberant environment, such as in a reverberation chamber. Thus, a standing $\mathrm{sinc}(kx)$ wave is ideally created at every TR focus location for each frequency. The authors found good agreement between experimental results of TR focusing at multiple locations when compared to standing wave $\mathrm{sinc}(kx)$ functions being superposed at those same relative locations in a theoretical model. This approach may be used to understand why the magnitude of the frequency spectrum deviates from the desired focused noise, such as white noise; in other words, it explains why the dips occur and the frequency at which they occur.

Figure 3.5 illustrates two standing $\mathrm{sinc}(kx)$ functions located a distance d apart. These figures show the interaction of three arbitrary frequencies in the spatial domain, highlighting how $\mathrm{sinc}(kx)$ standing waves influence wave focusing. In Fig. 3.5(a), when lower frequency foci are

closely spaced, the main lobes at the two focal points interact constructively, reinforcing each other. The maximum constructive interference possible, occurring when they focus at the same location, is a 6 dB gain. In contrast, Fig. 3.5(b) shows that if the standing waves are spaced so that the main lobe of one aligns perfectly with the deepest trough of the other, it results in destructive interference at each of the two focal points for that frequency. The expected amount of destructive interference for Fig. 3.5(b) is a 2.1 dB reduction of each focal peak. This derives from taking the difference in amplitudes between the peak (amplitude value of 1) and the trough amplitude of the sidelobe (-0.217) of the other focus resulting in a peak of only 0.783 and comparing it to an amplitude of 1.0 as a dB value. Adding a third focus location spaced the same distance away would double that amplitude decrease for the middle focus location to a 4.3 dB reduction with appropriate rounding. The frequency that results in this maximal destructive inference (the frequency of the dip), f_d, is

$$f_d = 0.715\frac{c}{d}, \tag{3}$$

where c is the speed of sound. The constant 0.715 derives from the location of the largest trough of the $\mathrm{sinc}(kx)$ function relative to a wavelength. Finally, Fig. 3.5(c) demonstrates that when the focal points are sufficiently spaced apart relative to a wavelength, there is minimal interference between the two foci; this allows the standing waves to essentially behave independently, with little interaction between them.

It is acknowledged that the spatial correlation function for a diffuse field environment is modeled by the $\mathrm{sinc}(kx)$ function.[31] While the $\mathrm{sinc}(kx)$ also represents single frequency focusing, the potential relationship between the two phenomena has neither been addressed nor investigated in this paper.

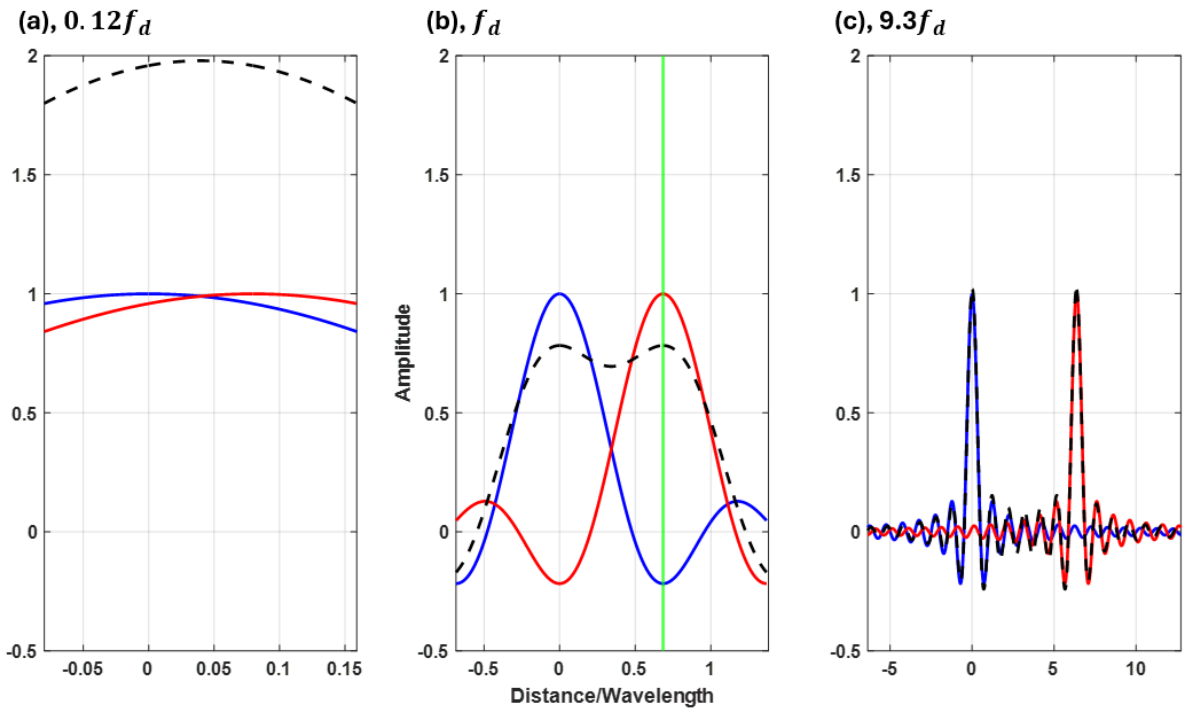

FIG. 3.5. Interaction of standing $sinc(kx)$ *functions located a scaled distance of* $0.715\frac{c}{f_d}$ *apart at three frequencies. (a) Close spacing leads to constructive interference. (b) Alignment of a peak with a trough causes destructive interference. (c) Sufficient spacing minimizes interference, allowing independent wave behavior at a frequency* $9.3f_d$*. The black dashed line represents the summed results between the two standing waves in each plot.*

When standing $\mathrm{sinc}(kx)$ waves interfere with each other, it results in the deviation of the spectrum from the target spectrum (white noise); this is further demonstrated in the next study. The goal of this study is to explore the effect of changing the span of foci while keeping the number of foci fixed. Figure 3.6 presents results where each case has 11 foci, with equal spacing between adjacent foci for each result. The foci are always centered around the 0.75 m mark for all span lengths. The span lengths explored are as follows, but only the **bolded** results are shown in Fig.

3.6: **150 cm**, 135 cm, 120 cm, 105 cm, 90 cm, **75 cm**, 60 cm, 45 cm, 35 cm, **30 cm**, 20 cm, 15 cm, **10 cm**, 5 cm, and a single-point focus. The other results are visible in an animation that progressively shows the results, which is shown in Mm. 2.

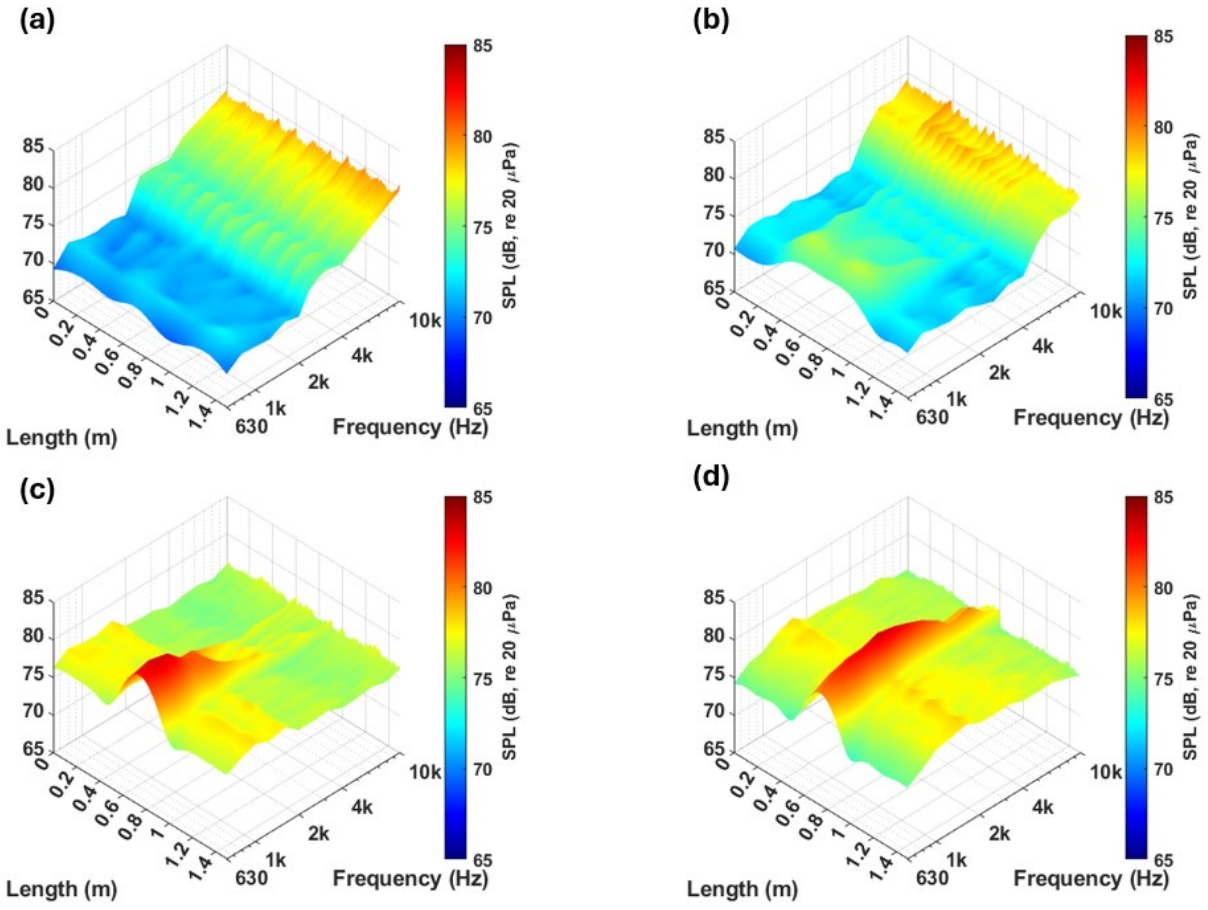

FIG. 3.6. Sound pressure level as a function of space and frequency, plotted as 1/3rd octave levels. This second study explores the effect of changing the density of foci across different span lengths while keeping the number of foci fixed at 11. The scanning grid covers 1.5 m, with the span of foci changing from (a) 150 cm, (b) 75 cm, (c) 30 cm, to (d) 10 cm spacing.

Mm. 2. Animation of the progression as the span of a fixed number of focal locations decreases from 150 cm, 135 cm, 120 cm, 105 cm, 90 cm, 75 cm, 60 cm, 45 cm, 35 cm, 30 cm, 20 cm, 15 cm, 10 cm, 5 cm, and a single-point focus. This is a file of type ".mp4" https://youtu.be/Rt-a_3y7qOo (0.165 MB).

From plots (a) to (b) in Fig. 3.6, the 630 Hz to 1600 Hz 1/3rd octave band levels increased in amplitude due to constructive interference, as the span length decreased from 150 cm to 75 cm. This constructive interference when the wavelength is larger than the spacing of occurred at progressively higher frequencies as the span length decreased. The 2500 Hz to 4000 Hz 1/3rd octave band levels from again plots (a) to (b) in Fig. 3.6 exhibit the dip in amplitude, reflecting a situation more akin to Fig. 3.5(b). Beyond the 4000 Hz 1/3rd band moving from plots (a) to (b) in Fig. 3.6, the frequencies seem unaffected by interference from other foci, like the scenario depicted in Fig. 3.5(c). As the span length and thus spacing between each foci decrease further, as in Fig. 3.6(c), the lower frequencies begin to gain in relative amplitude, while the frequencies above the 2000 Hz 1/3rd octave band are lower in level than desired. Finally, in Fig. 3.6(d), nearly all frequencies begin to constructively interfere with each other essentially as a single point focus. The animation, Mm. 2, illustrates the progressive changes as the spacing of foci becomes favorable, unfavorable, or neither in relation to the amplitude changes for each frequency band. It is apparent that the only scenario that does not significantly alter the desired frequency spectrum is the single point focus. This idea will continue to be discussed and analyzed in Section 3.3.2.

When performing the TR backward step for these second study results, a spacing of 1 cm between spatial measurement locations is maintained for every scan. However, in one experiment involving a 5 cm span length of foci, the spacing between each focus location needed to be smaller

than 1 cm. To create this spacing of foci of only 0.5 cm within the 5 cm target span length, the IRs were collected at the proper 0.5 cm spacing in the forward step, but the spatial measurement sampling during the scan of the TR backward step was maintained at a spatial resolution of 1 cm.

3.3.2 Two-dimensional scans

Increasing the spatial extent of multipoint focusing in 2D is now discussed. For this study, the scanning system is moved both horizontally and vertically to experimentally collect data from a 2D grid of chirp responses (CR) for 8 loudspeakers. This grid of CR data is then converted to a grid of IR signals using cross correlations. The grid of IR signals is used to simulate the spatial dependence of various TR backward step configurations. Here again, the broadcast signals are noise signals with a desired spectrum convolved with equalized TRIRs. The backward step propagation was simulated in MATLAB, by convolving each of the 8 broadcast signals (one for each loudspeaker) with the corresponding IR at every grid location. The convolved time signals corresponding to each loudspeaker broadcast were summed, essentially creating a single, cumulative recording, to produce the dataset used for analysis. In this study, since the backward step was simulated, the amplitude scale is relative and the absolute levels attained lack physical meaning, though relative differences in level can still be observed and learned from. The initial analysis includes one experiment for 2D scans that vary the density of foci within a given target region. White noise, with frequency content ranging from the 63 Hz to 10 kHz 1/3rd octave band frequencies, was consistently used in all experiments for the initial analysis.

Shown in Fig. 3.7, the total size of the scanning grid is 48 cm by 48 cm (the black colored region) and the target region for the following set of experiments is 24 cm by 24 cm (the red

colored region). The blue dots represent the focal location configurations, which include 1, 4, 9, 25, and 169 foci. Many more focal configurations within the target region could have been chosen but the ones studies here are configured to have equal spacing between adjacent foci in a square lattice of foci.

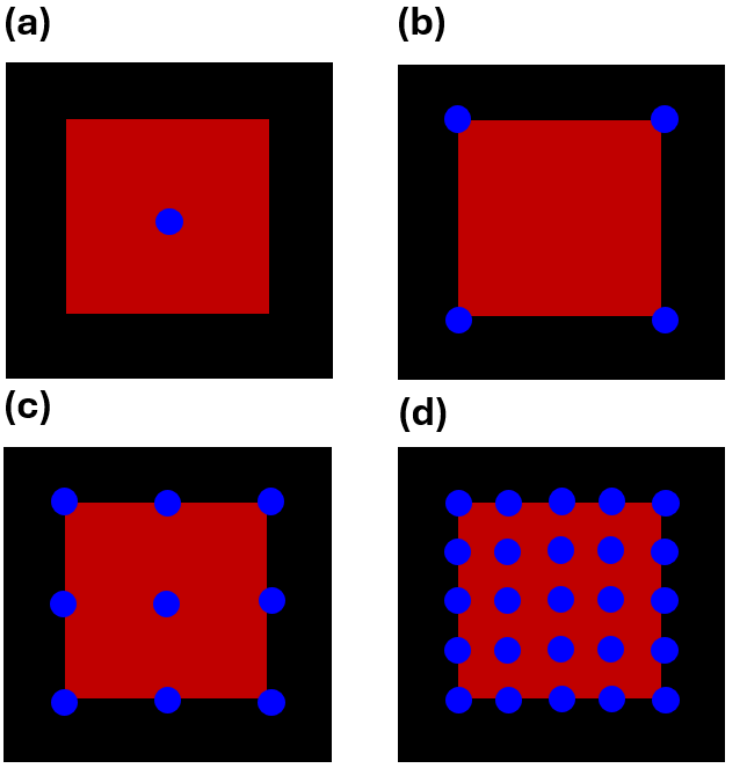

FIG. 3.7. The scanning grid (48 cm x 48 cm, black) and target region (24 cm x 24 cm, red) for a 2D configuration of foci. Blue dots indicate focus locations (1, 4, 9, 25) with equal spacing between adjacent foci.

For ease of interpretation, the amplitude values in the plots of this section have been adjusted by scaling them according to the bandwidth of each corresponding 1/3rd octave band. Instead of using the standard 1/3rd octave scaling, each frequency band's amplitude is divided by its bandwidth. This adjustment would result in a flat spectrum for white noise. The frequency axis

will still display data points corresponding to the 1/3rd octave band center frequencies. Unless otherwise specified, this scaling approach will be used throughout the remainder of this paper.

The first metric explored quantifies relative amplitude gains over the spatial extent of the 2D target region in terms of a spatially averaged amplitude for each focal configuration. For each spatial location within the target region, the 1/3rd octave band levels were calculated and scaled. The spatially averaged amplitude was then computed for each frequency across the target region. Figure 3.8(a) presents the spatially averaged amplitude for seven focal configurations of focusing white noise within the target region, overlaid with the result for broadcasting equalized white noise without TR from the same number of loudspeakers. As the number of foci increases, the lower frequency content shows a noticeable increase in amplitude, while higher frequency content may perform worse than simply broadcasting white noise without TR. It is again noted that the desired outcome is a flat spectrum (white noise). The problem is that the $\mathrm{sinc}(kx)$ interference, discussed in Section 3.3.1, is not being accounted for in the equalization for the TR focal configurations. It is important to emphasize that these plots represent spatially averaged amplitude, which explains the observed decrease in amplitude as frequency increases. Higher frequencies produce a narrower foci spatially, resulting in a lower spatially averaged amplitude compared to lower frequencies that have a larger focal width due to their longer wavelength. Adjusting the target region size would also impact the spatially averaged amplitude results: a smaller target area would result in higher frequencies averaging to a higher amplitude. Using Eq. (3) the calculated frequencies at which 4, 9, 25, and 169 foci have $\mathrm{sinc}(kx)$ dip interference are as follows, 1,021 Hz, 2,044 Hz, 4,087 Hz, and 12,262 Hz, respectively. These dips are each denoted by a star in Fig. 3.8(a), except for the 169 foci configuration due to the $\mathrm{sinc}(kx)$ interference dip happening at a frequency outside of the bandwidth.

The $\mathrm{sinc}(kx)$ interference dip could be addressed by calculating the difference between the desired spectra and the initially obtained averaged spectra, which did not account for the interference. This correction is applied now in MATLAB by adjusting all the 'broadcast signals' using the calculated difference (adjusting the already equalized signals further by equalizing to correct for the interference dip). The experiment is then repeated with the necessary equalizations to obtain the desired spectra. Figure 3.8(b) presents the spatially averaged amplitude for the properly equalized signals across various focus configurations. It is evident that the amplitude gains have now significantly decreased for every configuration, with the maximum achievable gain being roughly only 2 dB when compared to broadcasting white noise. The decrease in gains is a consequence of normalizing the signals to be broadcast from each loudspeaker by their peak values to maximize the input signal amplitude sent to each loudspeaker, thus resulting in a quasi-conservation of energy tradeoff. Accounting for the interference dip in the equalization eliminates the gains that are hoped for by using multipoint focusing with TR.

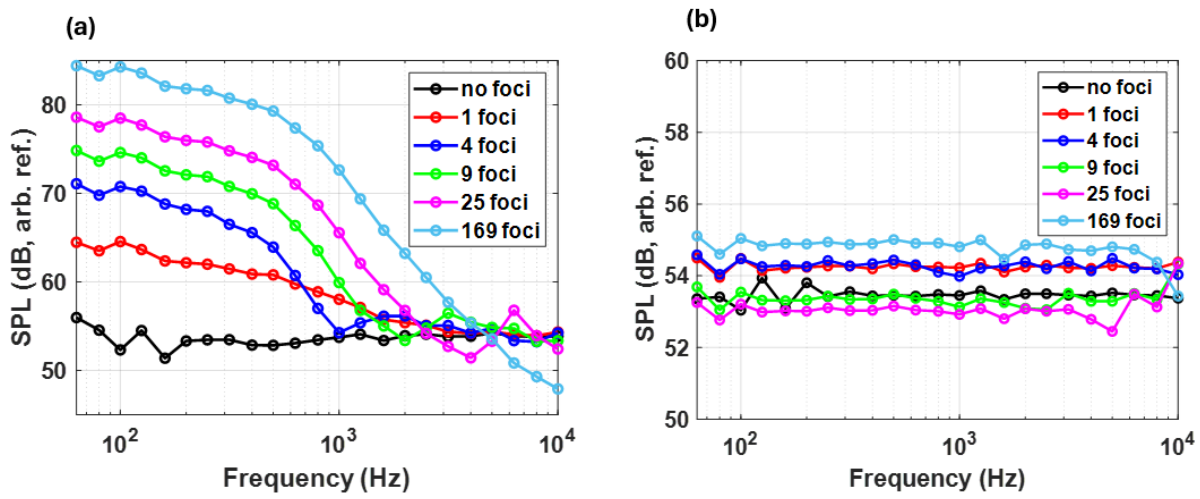

FIG. 3.8. (a) Spatially averaged amplitudes across the target region for different focal configurations along with a non-focusing scenario (a) while not accounting for $\mathrm{sinc}(kx)$ *interference and (b) when accounting for the* $\mathrm{sinc}(kx)$ *interference.*

Figure 3.9 provides a different perspective on understanding the $\mathrm{sinc}(kx)$ interference correction through calculation of the OASPL for each spatial location in the grid. Figures 3.9(a) and (b) show the OASPL across the full 2D grid for 9 focal locations, both with and without equalization for $\mathrm{sinc}(kx)$ interference, while Figs. 3.9(c) and (d) present the same comparison for 4 focal locations. Without the $\mathrm{sinc}(kx)$ interference correction, the OASPL levels appear more rounded, with small spikes protruding slightly. However, when the $\mathrm{sinc}(kx)$ interference correction is applied, these spikes become more pronounced. This is expected, as without the correction, lower frequencies dominate the space while higher frequencies are reduced. By applying the correction, the higher frequencies are balanced with the lower frequencies, resulting in the correct spectral shape, but at the expense of the pronounced spikes that result from high

frequency content that have a smaller spatial extent of their focusing. The pronounced spikes indicate that the target region does not have a spatially uniform distribution.

While correcting the $\mathrm{sinc}(kx)$ interference successfully achieves the desired spectrum over the target region, the downside is that the amplitude gain remains minimal, and the spatially uniform excitation is compromised. This is an apparent inevitable tradeoff that cannot be avoided. To effectively compensate for the $\mathrm{sinc}(kx)$ interference while preserving the amplitude gains from TR, maintaining a spatially uniform excitation, and achieving the desired spectral shape, a different metric must be considered.

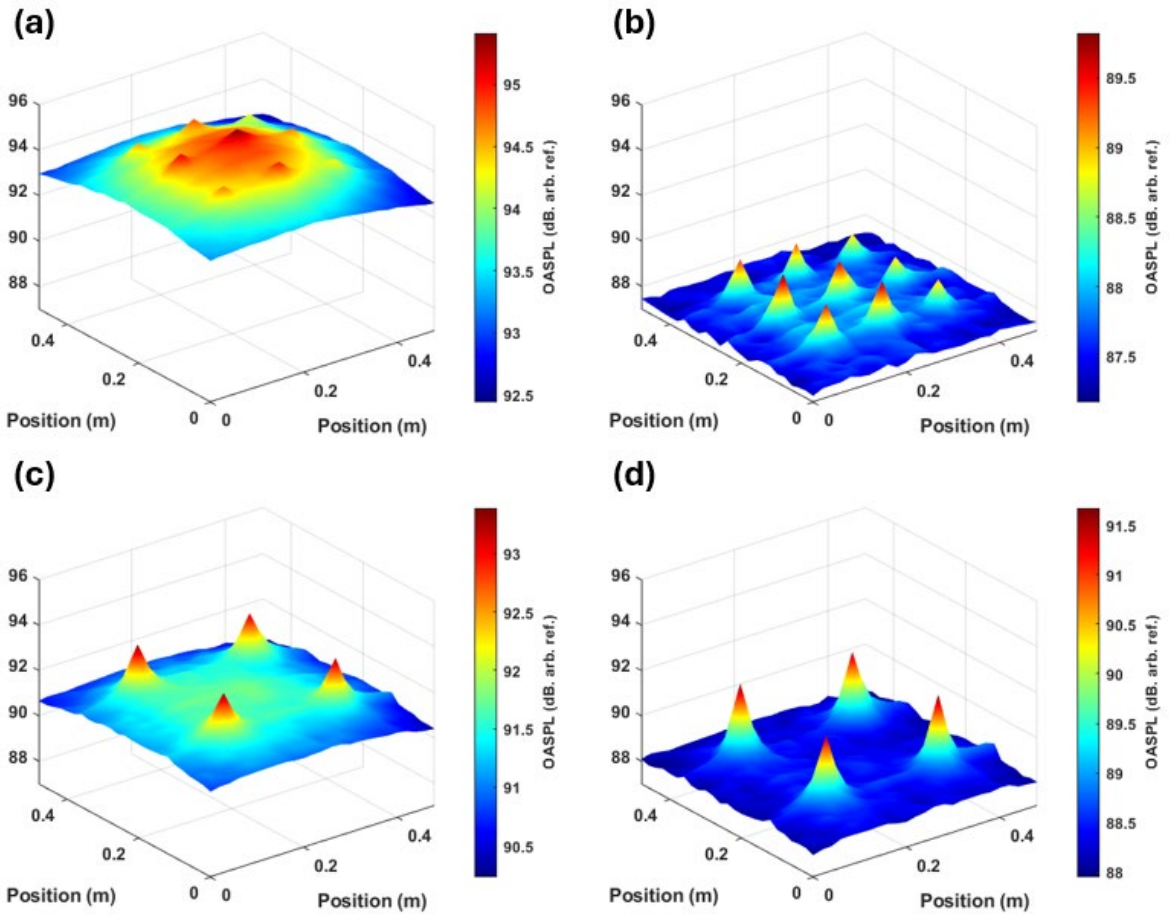

FIG. 3.9. Overall sound pressure level (OASPL) distribution across a 2D grid for different multi-focusing scenarios, comparing results with ((b) and (d)) and without ((a) and (c)) sinc(kx) interference correction. (a) and (b) show the OASPL for 9 focus locations, while (c) and (d) show results for 4 focus locations.

The next metric assesses the spatial variation (rather than the sum over space) within the spatial region of interest (target region) for the case of focusing noise with TR. It is desirable for the intended use case is to have the amplitudes over all of the target region be within 3 dB from the maximum value. To start off, for each frequency band, the 1/3rd octave band levels over the target

region are normalized by setting the maximum value to zero. The percentage of values among the target region that are within 3 dB of the maximum level is determined, which provides a measure of the variation in level over space. This percentage is computed for each 1/3rd octave band frequency and focal configuration, allowing for a comparison of the spatial variation of sound energy across various focusing scenarios.

Figure 3.10 illustrates the spatial variation percentage across different focusing scenarios. While it may not be immediately apparent which scenario performs best, some trends can be observed from the plot. Notably, all focusing scenarios show that 100% of the target region falls within the -3 dB tolerance up to the 400 Hz 1/3rd octave band. Above 400 Hz, the spatial variation of the single focus drops off, as expected, due to the narrowing of the main lobe of the standing $\mathrm{sinc}(kx)$ wave at higher frequencies. The other multi-point focusing variations seem less predictable, but the results can be attributed to the interference patterns of the individual $\mathrm{sinc}(kx)$ standing waves at each focus location. One particular focus variation, the 4-focus scenario, manages to maintain 100% of the target region within the -3 dB range up to the 800 Hz band. This observation was noted but not explored further. Given that significant spatial variations exist above 400 Hz, there seems to be little benefit in attempting to focus frequencies above 400 Hz for this target region.

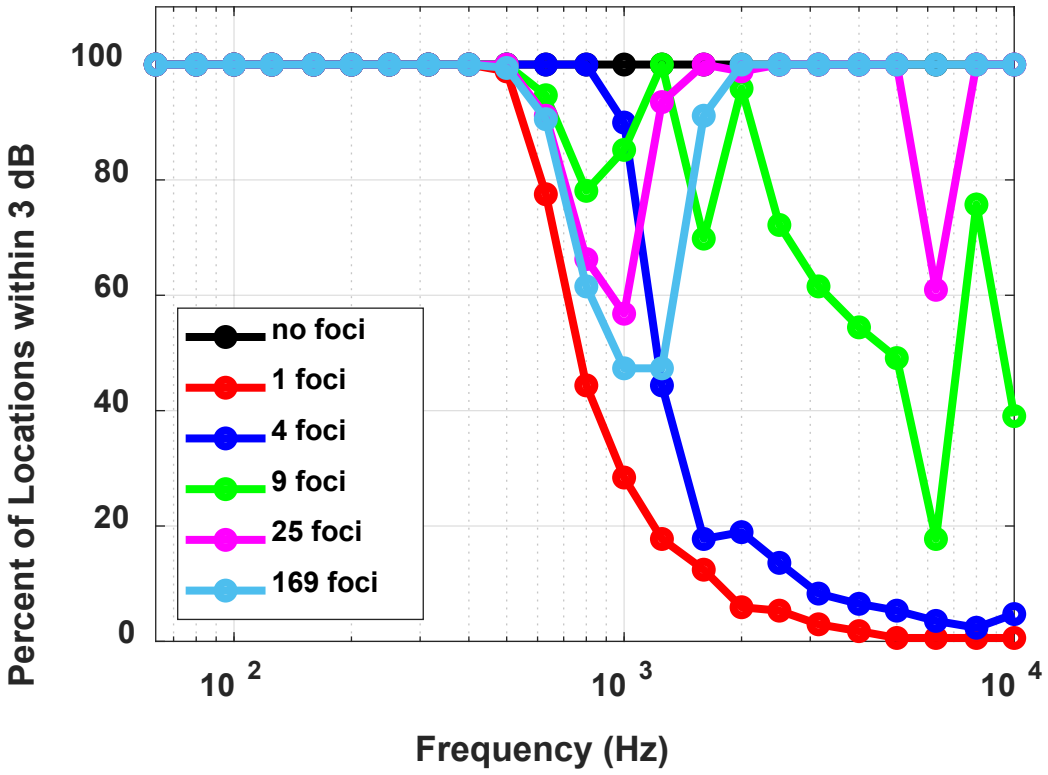

Fig. 3.10. Spatial variation analysis within the 2D target region (24 cm by 24 cm) for different 2D focusing scenarios (1, 4, 9, 16, 25, 49, 169 focus points). For each frequency band, the spectral data is normalized by setting the maximum amplitude to zero, and the percentage of values that deviate by more than −3 dB of the peak value within the focus region is calculated.

The average spatial amplitude for focusing white noise with a bandwidth of 63 Hz to 400 Hz 1/3rd octave frequency bands was determined. It is important to note that the expected $\mathrm{sinc}(kx)$ interference is accounted for in this case, whereas it was not accounted for in the results in Fig. 3.8(a). Each focus configuration was directly compared to the baseline results obtained from broadcasting white noise without TR across the same bandwidth. This ensures that all

configurations were assessed relative to the broadcast of white noise without TR under equivalent conditions, allowing for consistent comparison across all configurations. As shown in Fig. 3.11, the findings reveal a significant amplitude gain of at least 9 dB across all frequency bands for the focus configurations, compared to broadcasting white noise. In contrast, for the broader 63 Hz to 10 kHz bandwidth in this target region (shown in Fig. 3.8(b)), the previously observed maximum amplitude gain was only 2 dB. The only variable change between these scenarios (Fig. 3.8(a) vs. Fig. 3.11) was the decrease in bandwidth, which aligns with earlier findings in the spatial variation analysis. By not broadcasting the frequencies above the 400 Hz band, there is a corresponding apparent gain for the lower frequencies for the no TR case and and even greater gain for the TR cases (note the increase in the average levels shown in Fig. 3.11 versus those in Fig. 3.8(a)). It is important to stress that the reduction in bandwidth impacts some of the TR focal configurations more than others. Interestingly, all TR focus configuration produced very similar level outcomes. Based on this information, it is recommended that using a single-point focus under the current conditions is just as effective as any of the other focus configurations. The current conditions refer to the specific target area and bandwidth. The next section will provide a detailed explanation of how to achieve these amplitude gains of over 9 dB for a use case scenario.

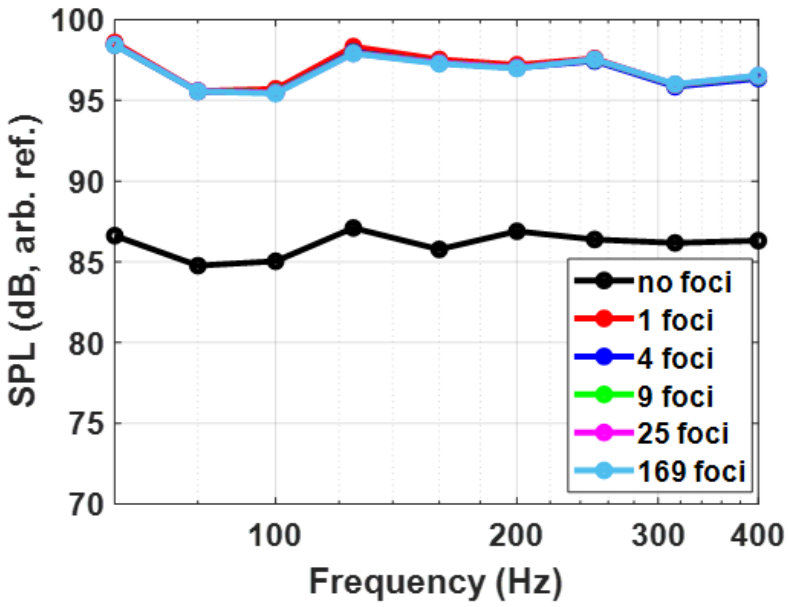

FIG. 3.11. Average spatial amplitude within the target region (24 cm by 24 cm) for a 1/3rd octave frequency bandwidth from 63 Hz to 400 Hz, while also accounting for $\mathrm{sinc}(kx)$ *interference for various time reversal (TR) foci configurations compared to not using TR. The arbitrary dB reference in Fig. 3.8 was also used in this figure.*

3.3.3 Use case of time reversal with long-duration noise signals

Using TR to focus noise for a use case scenario to achieve maximum gains, maximal spatial uniformity, and maintaining the desired spectral shape will now be discussed. A single TR focus location only will be explored due to the finding that an unavoidable tradeoff exists when focusing at multiple locations in that spatial uniformity cannot be achieved simultaneously with the desired spectral shape, all while still achieving gains in amplitude due to using TR. Fortunately the use of

a single focal location helps simplify the processing by decreasing the required measurements of IRs to be made up front. The need to only measure a single IR per loudspeaker is significant in terms of reducing the amount of equipment needed from a practical standpoint. The first thing that needs to be considered is the target area. The target area, which in some cases is the size of the structure, is what ends up directly determining the usable bandwidth that can be used to focus noise with TR and achieve maximum efficiency and spatial uniformity. Lower frequencies have a larger main lobe width for their corresponding standing $\mathrm{sinc}(kx)$ wave. The standing $\mathrm{sinc}(kx)$ wave model can be used to help determine the highest usable frequency for a specific target area. The goal is to identify the distance away from the peak at which the $\mathrm{sinc}(kx)$ function is greater than 0.707 (3 dB down from the peak) for each frequency, which will be referred to as the maximum target area radius, shown in Fig. 3.12. This can also be thought of as half the full width at half maximum distance for the squared $\mathrm{sinc}(kx)$ function. Figure 3.12 can be used to find the highest usable frequency for a specific target area that allows TR to focus noise with maximum efficiency and have the spatial distribution of amplitudes stay within -3 dB from the peak value.

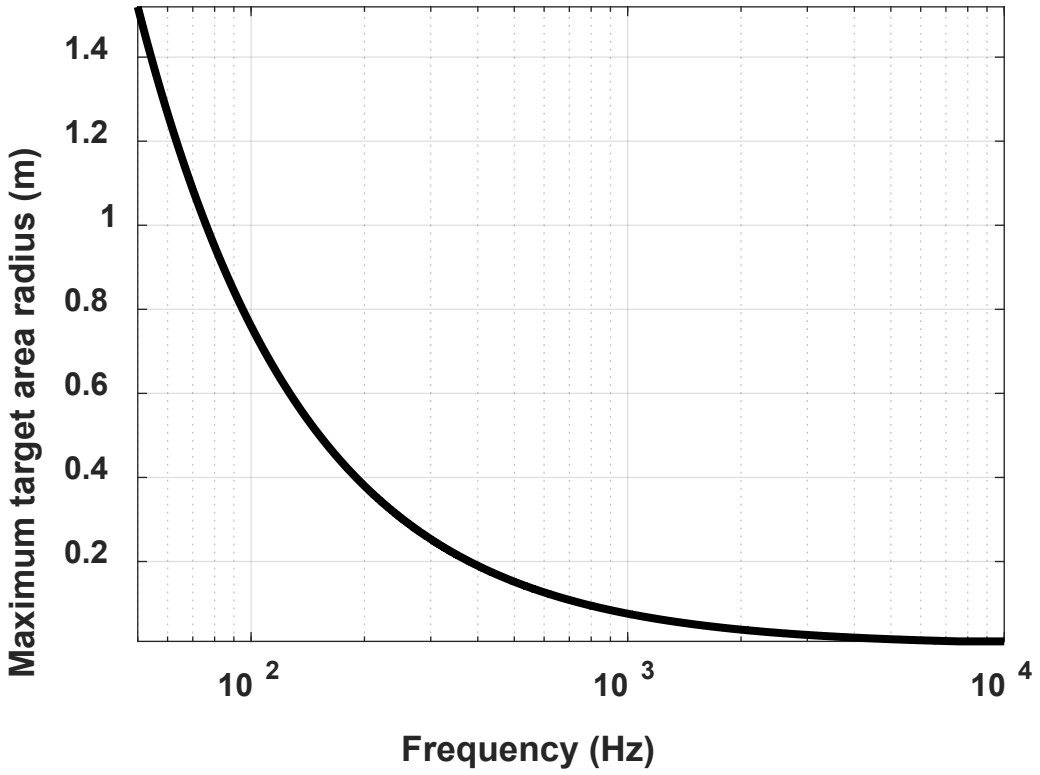

FIG. 3.12. The plot illustrates the tradeoff between the size of the optimal target area for single point time reversal focusing versus the frequency upper limit of the bandwidth of frequencies that will have optimal spatial uniformity over the target region. The $\mathrm{sinc}(kx)$ *function width is computed for a range of distances (0.01 m to 1.6 m).*

In Fig. 3.13, the red square represents the target area of 24 cm by 24 cm discussed earlier. To determine the distance from the center of this area to its corner we applied the Pythagorean theorem; this distance is depicted by the black line in the figure. The blue circle illustrates the size of the 2D Cardinal sine standing wave's main lobe that remains above the -3 dB threshold. The calculated distance of 0.17 m determines the highest frequency, that can be used in the bandwidth

to maintain spatial uniformity, to be 447Hz (using Fig. 3.12) which is contained within the 400 Hz 1/3rd octave frequency band. If frequencies are used above 447 Hz it will result in amplitudes being more than 3 dB down from the peak, resulting in undesirable spatial variation in the target area. The bandwidth of frequencies used can be increased while maintaining the desired spatial uniformity, but the target area must be decreased according to the guidelines in Fig. 3.12.

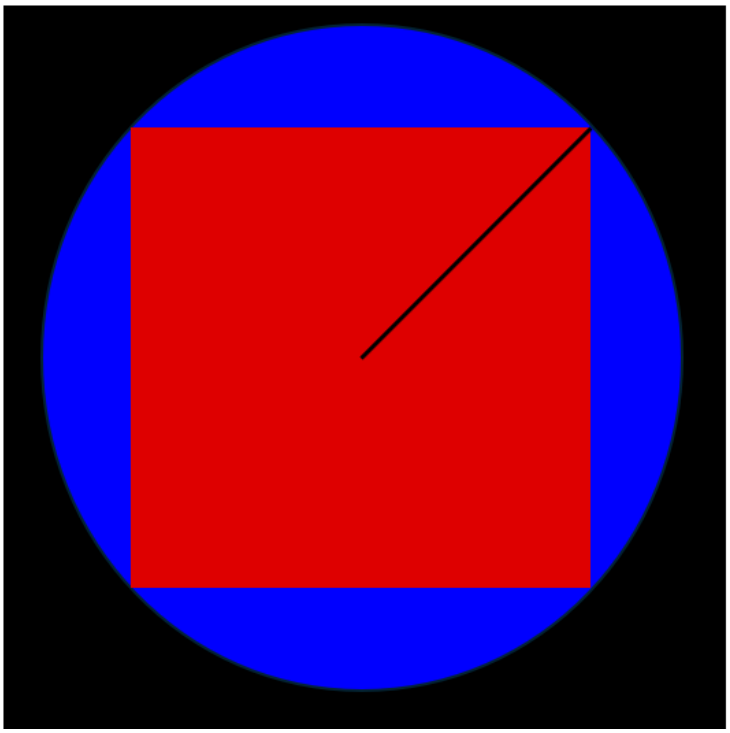

FIG. 3.13. The red square represents the 24 cm by 24 cm target area, with the blue circle showing the area of the highest frequency 2D Cardinal sine standing wave that is above the -3 dB threshold. The black line indicates the distance from the center to the corner of the target area, which is used to identify the highest usable frequency.

Focusing noise to different target areas using a single focus location is now examined. The target areas considered include 8 cm by 8 cm, 12 cm by 12 cm, 24 cm by 24 cm, and 32 cm by 32

cm with maximum distances from the center measuring 5.7 cm, 8.5 cm, 11.3 cm, and 22.6 cm, respectively. The noise band begins with the 63 Hz 1/3rd octave band frequencies, and the upper frequency limit is determined by the maximum distance from the center of each target area, which can be determined using Fig. 3.12. The corresponding final 1/3rd octave band center frequencies for these distances are 1000 Hz, 800 Hz, 400 Hz, and 315 Hz, respectively. Notably, as the target area decreases, higher frequency content can be effectively focused with maximum amplitude gains while maintaining spatial uniformity and the desired spectral shape. Figure 3.14 presents the average spatial amplitude results for the different target regions, using their respective bandwidths to focus white noise. The results in Fig. 3.14 demonstrate a minimum 9 dB increase in amplitude when focusing white noise with TR compared to broadcasting white noise without TR across all target areas.

So far, only white noise has been considered. To expand the analysis, a spectrum specified in a standard[32] shown in Fig. 3.15, represented by red-colored diamond markers, was used with the same focusing process applied to white noise. This test was conducted using one of the previous target areas, specifically 24 cm by 24 cm. Given the target area, the frequency band used was 63 Hz to 400 Hz in 1/3rd octave frequency bands. The results in Fig. 3.15 show that it is possible to focus different shaped spectra of noise and still achieve significant amplitude gains when using TR compared to not using TR. The spectra shown in Fig. 3.15 are on a 1/3rd octave frequency band scale that are not scaled by its corresponding band.

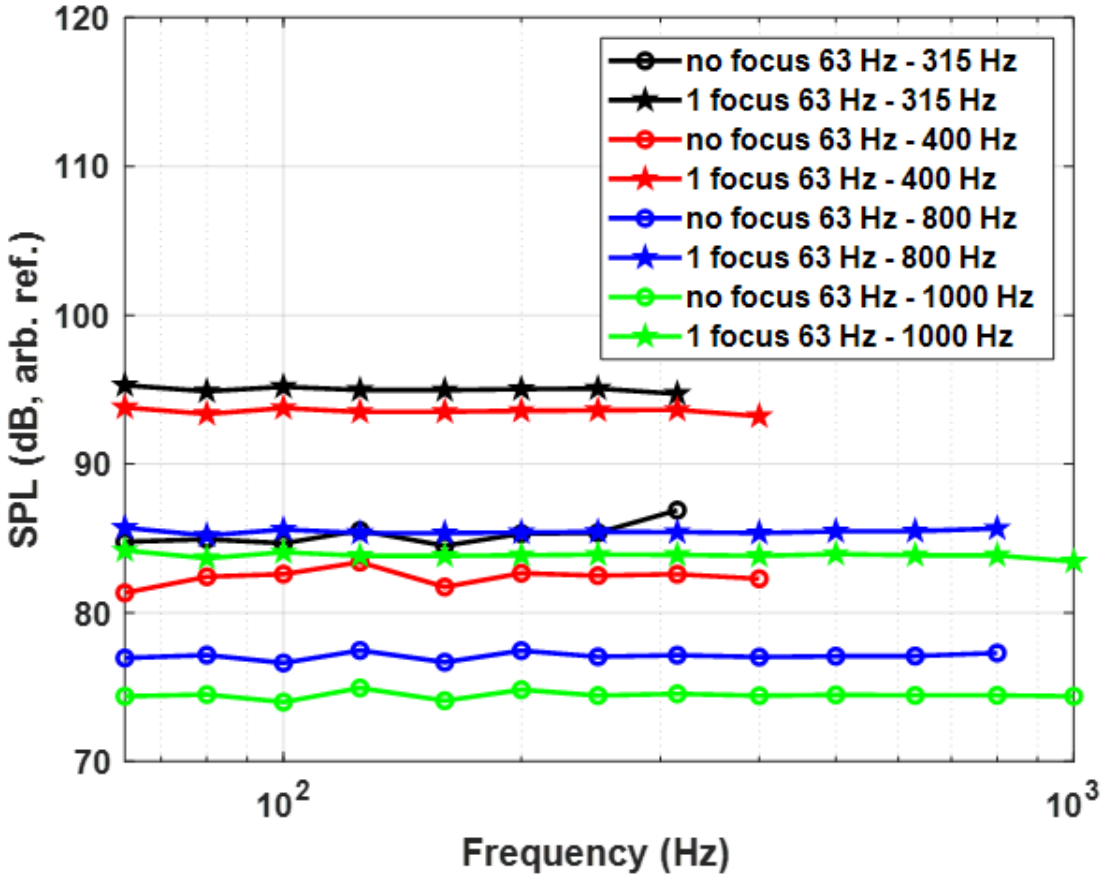

FIG. 3.14. Focusing noise with time reversal (data with star markers) compared to broadcasting noise without time reversal (data with circle markers). Average spatial amplitude results for different target areas, each using their respective optimal bandwidths to focus white noise. The target areas considered are (black) 32 cm by 32 cm, (red) 24 cm by 24 cm, (blue) 12 cm by 12 cm, and (green) 8 cm by 8 cm. The arbitrary dB reference in Fig. 3.8 was also used in this figure.

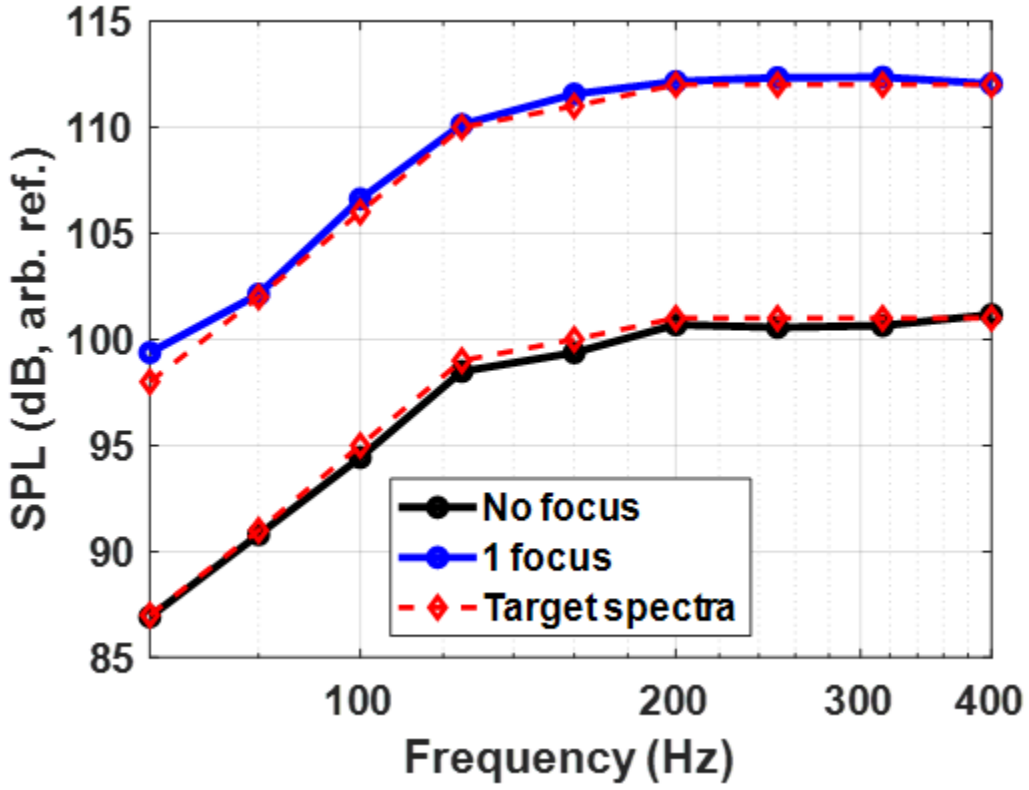

Fig. 3.15. Average spatial amplitude of a single time reversal focus of noise (blue) having the spectral shape as defined by a standard compared to not using time reversal (black). The red curve represents the shape of the desired spectrum, whose amplitude is scaled to fit both cases to facilitate comparison of the desired spectral shape to the resulting spectral shapes. The arbitrary dB reference in Fig. 3.8 was also used in this figure.

3.4 Conclusion

This study investigated the spatial extent of time-reversal (TR) focusing for long-duration broadband noise signals by varying the density of focal points and measuring their effects on overall sound pressure level (OASPL) and spectral shape when focusing in a line along 1D. The results showed that higher focal densities produced more uniform OASPL distributions, while lower densities led to distinct peaks. However, in the frequency domain lower focal densities achieved the desired spectral shape but with uneven OASPL spatial distribution, while higher densities provided more uniform OASPL spatial coverage but deviated more from the desired noise spectrum. These deviations seem to result from standing $\mathrm{sinc}(kx)$ waves at each focus location that interfere with adjacent foci, which distorted the intended spectra. Similar issues arose in 2D multi-focusing experiments, regardless of focal variation (changing the density) within the intended target area. Application of an additional equalization step, used to remove the effects of $\mathrm{sinc}(kx)$ interference, corrected the spectra but also resulted in larger deviations in levels spatially across the target spatial region.

It was determined that if a single TR focus is created and the bandwidth is limited, the spatial variations can be minimized over a known area (the full width at half maximum of the 2D Cardinal sine function). Within this minimized bandwidth, TR provided a 9 dB gain over not using TR and it was also shown that it is possible to preserve the desired spectral shape and spatial uniformity in the TR focusing. For practical applications, a single-point focus with an upper frequency limit (determined by the desired target area) can achieve equivalent amplitude gains to multi-focus configurations. This approach is practically advantageous because it simplifies the process by requiring only one impulse response (IR) per loudspeaker, rather than multiple IRs per

loudspeaker. The target area dictates an upper frequency limit, as it is desired to maintain amplitudes within this area to be no less than –3 dB from the maximum value, reducing spatial variation, while also maintaining the desired spectrum.

3.5 References

[1] M. Fink, "Time reversed acoustics," *Phys. Today* **50**(3), 34-40 (1997).

[2] B. E. Anderson, M. Griffa, C. Larmat, T. J. Ulrich, and P. A. Johnson, "Time reversal," *Acoust. Today* **4**(1), 5–16 (2008).

[3] M. Fink, G. Montaldo, and M. Tanter, "Time-reversal acoustics in biomedical engineering," *Annu. Rev. Biomed. Eng.* **5**, 465–497 (2003).

[4] J. V. Candy, A. W. Meyer, A. J. Poggio, and B. L. Guidry, "Time reversal processing for an acoustic communications experiment in a highly reverberant environment," *J. Acoust. Soc. Am.* **115**(4), 1621–1631 (2004).

[5] C. S. Clay and B. E. Anderson, "Matched signals: The beginnings of time reversal," *Proc. Meet. Acoust.* **12**(1), 055001 (2011).

[6] B. E. Anderson, T. J. Ulrich, P.-Y. Le Bas, and J. A. Ten Cate, "Three dimensional time reversal communications in elastic media," *J. Acoust. Soc. Am.* **139**(2), EL25-EL30 (2016).

[7] C. Song, "An overview of underwater time-reversal communication," *IEEE J. Oceanic Eng.* **41(**3), 644–655 (2016).

[8] B. E. Anderson, M. C. Remillieux, P.-Y. Le Bas, and T. J. Ulrich, "Time reversal techniques," Chapter 14 in *Nonlinear Acoustic Techniques for Nondestructive Evaluation, 1st Edition*, Editor Tribikram Kundu, ISBN: 978-3-319-94476-0 (Springer and Acoustical Society of America), pp. 547-581 (2019).

[9] S. M. Young, B. E. Anderson, S. M. Hogg, P.-Y. L. Bas, and M. C. Remillieux, "Nonlinearity from stress corrosion cracking as a function of chloride exposure time using the time reversed elastic nonlinearity diagnostic," *J. Acoust. Soc. Am.* **145**(1), 382–391 (2019).

[10] B. E. Anderson, R. A. Guyer, T. J. Ulrich, and P. A. Johnson, "Time reversal of continuous wave, steady-state signals in elastic media," *Appl. Phys. Lett.* **94**(11), 111908 (2009).

[11] B. M. Harker and B. E. Anderson, "Optimization of the array mirror for time reversal techniques used in half-space environment," *J. Acoust. Soc. Am.* **133**, EL351–EL357 (2013).

[12] G. Ribay, J. de Rosny, and M. Fink, "Time reversal of noise sources in a reverberation room," *J. Acoust. Soc. Am.* **117**(5), 2866-2872 (2005).

[13] C. Larmat, R. A. Guyer, and P. A. Johnson, "Tremor source location using time-reversal: selecting the appropriate imaging field," *Geophys. Res. Lett.* **36**(22), L22304 (2009).

[14] B. E. Anderson, M. Clemens, and M. L. Willardson, "The effect of transducer directionality on time reversal focusing," *J. Acoust. Soc. Am.* **142**(1), EL95–EL101 (2017).

[15] S. Yon, M. Tanter, and M. Fink, "Sound focusing in rooms: The time-reversal approach," *J. Acoust. Soc. Am.* **113**(3), 1533–1543 (2003).

[16] M. H. Denison and B. E. Anderson, "Time reversal acoustics applied to rooms of various reverberation times," *J. Acoust. Soc. Am.* **144**, 3055-3066 (2018).

[17] M. L. Willardson, B. E. Anderson, S. M. Young, M. H. Denison, and B. D. Patchett, "Time reversal focusing of high amplitude sound in a reverberation chamber," *J. Acoust. Soc. Am.* **143**(2), 696-705 (2018).

[18] B. D. Patchett and B. E. Anderson, "Nonlinear characteristics of high amplitude focusing using time reversal in a reverberation chamber," *J. Acoust. Soc. Am.* **151**(6), 3603-3614 (2022).

[19] M. Farin, C. Prada, and J. de Rosny, "Selective remote excitation of complex structures using time reversal in audible frequency range," *J. Acoust. Soc. Am.* **146**, 2510 (2019).

[20] M. Farin, C. Prada, T. Lhommeau, M. El Badaoui, and J. de Rosny, "Towards a remote inspection of jet engine blades using time reversal," *J. Sound Vib.* **525**, 116781 (2022).

[21] M. Tanter, J. Thomas, and M. Fink, "Time reversal and the inverse filter," *J. Acoust. Soc. Am.* **108**(1), 223–234 (2000).

[22] T. J. Ulrich, B. E. Anderson, P.-Y. Le Bas, C. Payan, J. Douma, and R. Snieder, "Improving time reversal focusing through deconvolution: 20 questions*," Proc. Meet. Acoust.* **16**, 045015 (2012).

[23] B. E. Anderson, J. Douma, T. J. Ulrich, and R. Snieder, "Improving spatio-temporal focusing and source reconstruction through deconvolution," *Wave Mot.* **52**, 151-159 (2015).

[24] A. D. Kingsley, A. Basham, and B. E. Anderson, "Time reversal imaging of complex sources in a three-dimensional environment using a spatial inverse filter," *J. Acoust. Soc. Am.* **154**(2), 1018–1027 (2023).

[25] B. E. Anderson, M. Griffa, T. J. Ulrich, and P. A. Johnson, "Time reversal reconstruction of finite sized sources in elastic media," *J. Acoust. Soc. Am.* **130**(4), EL219–EL225 (2011).

[26]A. D. Kingsley, J. M. Clift, B. E. Anderson, J. E. Ellsworth, T. J. Ulrich, and P.-Y. Le Bas, "Development of software for performing acoustic time reversal with multiple inputs and outputs," *Proc. Meet. Acoust.* **46**, 055003 (2022).

[27] M. R. Schroeder, "The 'Schroeder frequency' revisited," *J. Acoust. Soc Am.* **99**(5), 3240–3241 (1996).

[28] ISO 3741:2010, "Sound power and energy in reverberant environments," (International Organization for Standardization, Geneva, Switzerland, 2010).

[29] B. D. Patchett, B. E. Anderson, and A. D. Kingsley, "The impact of room location on time reversal focusing amplitudes," *J. Acoust. Soc. Am.* **150**(2), 1424-1433 (2021).

[30] D. Cassereau and M. Fink, "Time-Reversal of Ultrasonic Fields: Part III: Theory of the Closed Time-Reversal Cavity," *IEEE Trans. Ultrason. Ferroelectr. Freq. Control* **39**(5), 579–592 (1992).

[31] Pierce AD. Acoustics: An introduction to its physical principles and applications. Woodbury, New York): Acoustical Society of America; 1989. p.351.

[32] "MIL-STD-810G" (Department of Defense Test Method Standard, 515.6A-4 (2008)).

Chapter 4

Conclusion

Time Reversal (TR) delivery of noise signals provides a higher amplitude than not broadcasting noise without TR. At the focus location, the duration of the noise signal influenced the overall sound pressure level (OASPL), with longer durations resulting in lower OASPL. Doubling the number of loudspeakers that are broadcasting identical, synchronized noise signals led to an approximate ~6 dB increase in OASPL, when using TR, due to the coherent addition of the focused signals from each of the loudspeakers. An approximate ~3 dB, incoherent-addition increase was found when broadcasting the identical noise signals without the use of TR since nothing is being done to ensure coherent addition. It was found that TR delivery of noise can still result in a desired excitation spectrum with proper equalization. Depending on the spectral shape of the noise, the OASPL is influenced by the frequency content. In the reverberation chamber case explored here, lower frequencies contributed to a higher OASPL due to longer reverberation times at these frequencies.

Exploring the spatial extent of single and multipoint noise focusing using TR revealed trade-offs when varying focal point density. Higher densities of focal locations produced more uniform OASPL distributions, but this resulted in a deviation from the desired spectral shape, while lower densities of focal locations achieved the desired spectrum but resulted in distinct peaks and thus an uneven spatial distribution. The spectral deviations from multipoint focusing were caused by

interference from Cardinal sine standing waves at every focus location. The broadcasted signals can then be equalized to counteract the effects of this interference. It was concluded that an upper frequency band limit is necessary to achieve maximum amplitude gains of 9 dB when comparing the use of TR broadcasting versus non-TR broadcasting of noise, across various focal point variations within a given target area. Imposing this upper frequency band limit is necessary to ensure compliance with the desired spectral shape at frequencies below this limit. For the implementation of this method, a single-point focus was determined to be more effective than multiple-point focusing in achieving amplitude gain across a target area, provided the corresponding upper frequency limit is applied.

4.1 Implementation and limitations

Implementing TR with long-duration noise signals can be an effective method to acoustically excite a structure, whether for assessing and monitoring structural health or for replicating the acoustical environmental conditions a structure or object would experience in real-world applications. TR can be advantageous to use over traditional excitation methods because it allows for an increase in amplitude of about 9 dB for a given loudspeaker gain and number of loudspeakers. However, this method has its limitations. The primary limitation is the size of the spatial region that the desired noise will be delivered to while maintaining the desired spectrum shape. Consequently, the size of the target spatial region imposes a limit on the upper frequency of the desired spectrum. A key characteristic of using TR to deliver noise is that the gain in amplitude depends on the number of loudspeakers used; for every doubling of loudspeakers, an approximate 6 dB gain is achieved compared to the ~3 dB gain without the use of TR.

4.2 Future work

It is hypothesized that the focusing results observed in one plane would similarly occur in other planes. This is because when TR is implemented in a reverberation chamber with long impulse responses, the waves should converge spherically from all directions. Conducting a further experiment using TR with noise in three dimensions could confirm this hypothesis. This experiment would validate the findings of single-point focusing observed in two dimensions across multiple planes in 3D space.

TR delivery of noise of a desired spectral shape should be explored when the target focus location is on the side of a structure under test. By placing monitoring microphones around the focus location during structural testing, it can be determined whether the structure is receiving the desired spectral excitation within the tolerance desired (±3 dB for example) over the target region.

This thesis explored focusing of long-duration noise signals in air. Applications of this technique with noise in solids or liquids could be explored to determine if the observations made in air would hold true in other media. It is hypothesized that these findings would hold in other media, including solid media, though in solid media there are multiple wavelengths to consider.